SEMMELWEIS EGYETEM

DOKTORI ISKOLA

Ph.D. értekezések

3304.

KAKUK MELINDA

A gyógyszerészeti tudományok korszerű kutatási irányai

című program

Programvezető: Dr. Antal István, egyetemi tanár

Témavezető: Dr. Kállai-Szabó Nikolett, egyetemi docens

INNOVATIVE IN VITRO DISSOLUTION STUDIES FROM VARIOUS PHARMACEUTICAL DOSAGE FORMS AND VIS IMAGING USING ARTIFICIAL NEURAL NETWORKS

PhD thesis

Melinda Kakuk

Semmelweis University Doctoral School

Pharmaceutical Sciences Division

Supervisor: Nikolett Kállai-Szabó, Ph.D.

Official reviewers: Mirzahosseini Arash, Ph.D.

Péter Gieszinger, Ph.D.

Complex Examination Committee

Head of Committee: Romána Zelkó, D.Sc.

Members of Committee: Ildikó Kovácsné Bácskay, D.Sc.

Imre Klebovich, D.Sc.

Budapest

2025

Table of Contents

List of Abbreviations

API – Active Pharmaceutical Ingredient

ASD – Artificial Stomach-Duodenum

BA – Bioavailability

BCS – Biopharmaceutical Classification System

BE – Bioequivalence

Caco-2 – Human colorectal adenocarcinoma cells

CE – Cross entropy

CTAB – Cetyl-trimethyl-ammonium bromide

DC – Direct compression

DCS - Developability Classification System

DR – Delayed-release

EFT - Effervescent Floating Tablets

EMA – European Medicines Agency

FaSSCoF – Fasted State Simulated Colonic Fluid

FaSSGF - Fasted State Simulated Gastric Fluid

FaSSIF – Fasted State Simulated Intestinal Fluid

FaSSIF-V2 - Fasted State Simulated Intestinal Fluid version 2

U. S. FDA – The United States Food and Drug Administration

FEP – Fluorinated ethylene-propylene

FeSSCoF – Fed State Simulated Colonic Fluid

FeSSGF - Fed State Simulated Gastric Fluid

FeSSIF - Fed State Simulated Intestinal Fluid

FeSSIF-V2 - Fed State Simulated Intestinal Fluid version 2

GI – Gastrointestinal

GIT – Gastrointestinal tract

GRDDSs – Gastroretentive drug delivery systems

HCl – Hydrogen-chloride

HIA – Human Intestinal Absorption

HPLC – High Performance Liquid Chromatography

ICH – International Council for Humanization of Technical Requirements for Pharmaceuticals for Human Use

ICP-OES – Inductively Coupled Plasma Optical Emission Spectroscopy

IR – Immediate-release

IVIVC – In vitro-In vivo correlation

JP – Japanese Pharmacopoeia

lagT – Lag Time

LDAO – Lauryl-dimerhylamine-oxide

MR – Modified drug release

MWTA – Multivariate Wavelet Texture Analysis

NF – National Formulary

PDMS – Polydimethylsiloxane

PFA – Perfluoroalkoxyalkan

Ph. Eur. – European Pharmacopoeia

PP – Polypropylene

PRNN – Pattern recognition neural network

PSD – Particle size distribution

PTFE – Polytetrafluoroethylene

PVDF – Polyvinylidene fluoride

RMSE – Relative mean squared error

SCoF – Simulated Colonic Fluid

SGF – Simulated Gastric Fluid

SIF – Simulated Intestinal Fluid

SLS – Sodium lauryl sulfate

t_{max} – Time to maximum plasma concentration

UHMW PE – Ultra high molecular weight polyethylene

USP – United States Pharmacopeia

1 Introduction

1.1 The role of dissolution testing in the pharmaceutical industry

Dissolution testing in the pharmaceutical industry is used to predict expected bioavailability and for quality control purposes. The release of active pharmaceutical ingredients from dosage forms is examined throughout product development to determine the final formulation and in research to evaluate the impact of manufacturing parameters, as well as to assess the quality and quantity of excipients involved in the composition (1). Quality control is present from the early stages of development, ensuring that the product meets specified criteria at every manufacturing step. The methods used in quality control are simple, standardized, and well-regulated by pharmaceutical authorities. These tests help verify attributes like tablet content uniformity, disintegration time and drug release profile. In addition, stability testing of tablets plays an important role by comparing the dissolution profiles of drugs stored under certain conditions over time with those of the original samples.

Accurately predicting the in vivo bioavailability from a drug delivery system requires effective modeling of the gastrointestinal environment. Dissolution methods must simulate the biological environment, where the dosage form encounters varying pH, ionic strength and bile salt concentrations. Simulating these conditions in the laboratory is especially important for formulations with enteric coatings, where drug release in the stomach is undesirable. Per os administration, the first point of entry is the mouth, which in some cases (for example, sublingual tablets) is also the site of absorption. Beyond the mouth, the gastrointestinal tract is divided into three main sections: the stomach, the small intestine and the colon (2). The variable conditions of the GI tract significantly affect the in vivo dissolution profile of the active ingredient (API) (3), as the environment secretes various substances such as water, enzymes, surfactants and hydrochloric acid, which influence pH, buffer capacity and molarity (4). These factors collectively impact the dissolution and absorption of APIs (5). While both the stomach and small intestine play fundamental roles in the dissolution process, the small intestine is typically the primary site of absorption. Although some absorption occurs in the colon, its contribution is generally less significant than that of the small intestine.

Food and fluid intake, in addition to factors such as disease and concomitant medications, greatly influence the gastrointestinal environment. Therefore, in vitro bioavailability studies are performed under standardized conditions. According to European Medicines Agency (EMA) guidelines, bioequivalence (BE) studies are generally conducted in the fasting state, as this is considered the most sensitive condition for detecting differences between formulations (6). Similarly, the U.S. Food and Drug Administration (FDA) requires fasting studies for proving bioequivalence (7). Study participants typically fast for 8 hours before the administration of the drug delivery system, after which both test and reference preparations are given with a standard volume of water (240 ml). No food is allowed for at least 4 hours of post-dosing (8).

However, for many active ingredients, the bioavailability of conventional oral dosage forms is partly limited by rapid gastric emptying. Many active molecules benefit from prolonged gastric retention. Gastroretentive drug delivery systems (GRDDS) provide an optional solution to extend gastric residence time (9-11). Numerous technologies (such as floating systems, swelling systems, etc.) have been developed to increase the time a drug delivery system remains in the stomach (12).

1.2 The Biopharmaceutical Classification System (BCS)

From a bioavailability perspective, two major physicochemical properties characterize active ingredients: solubility and permeability. Studies have shown that these two factors are the most critical in the relationship between in vitro drug dissolution and in vivo bioavailability. Based on these properties, APIs can be classified into four groups (Figure 1) (13).

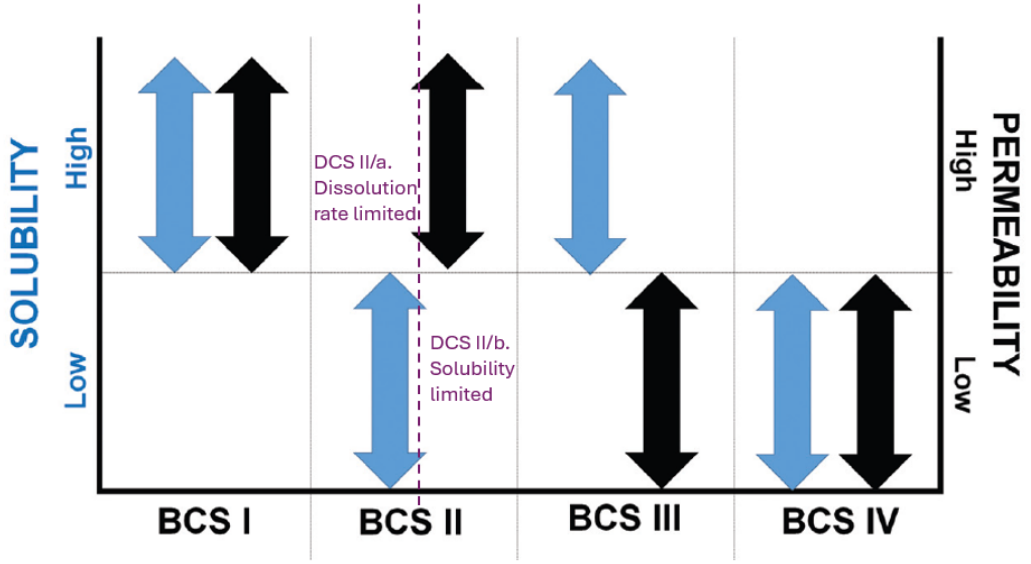

Figure 1 *The Biopharmaceutical Classification System (BCS) (own figure) Diagram of the BCS (Biopharmaceutics Classification System), which categorizes drug molecules into four classes based on their solubility and permeability. The diagram also includes the two subgroups of BCS Class II: DCS II/a. and DCS II/b.*

According to BCS, an active ingredient is considered highly soluble if its highest dose dissolves in 250 ml or less of aqueous medium at pH 1.0–7.5; otherwise, it is classified as poorly soluble (15). The 250 ml volume estimate comes from bioequivalence study protocols, which require patients to take a dosage form with a glass of water (16). The EMA specifies a pH range of 1.2–6.8 for solubility tests, requiring measurement of the aqueous medium's pH both before and after adding the API (17). The solubility of poorly soluble APIs can be improved by using solubilizing agents. Additionally, recent studies suggest that API permeability can also be modified by adding excipients to the formulation (18).

During early-stage drug candidate research, a molecule's physicochemical properties can be altered by modifying its chemical structure. Adding polar substituents (19) or using salt formation (20) can improve the water solubility of poorly soluble molecules, while lipophilicity can be enhanced, for example, by introducing a fluorine substituent. However, changing the chemical structure of a drug candidate is often impractical, as it may affect the compound's therapeutic efficacy, metabolism, toxicity, or synthesis.

Therefore, formulation techniques often provide a more favorable solution to poor water solubility.

Permeability classification is based directly on the API's human intestinal absorption (HIA). Good permeability is defined as a drug with greater than 85% absorption. An API is considered highly permeable if its absorption from the intestine reaches or exceeds 90%. If this property measures below 85%, the API is considered poorly permeable (21, 22). Current data show that about 70% of new drug molecules are poorly water-soluble, BCS Class II drugs, which presents significant challenges for pharmaceutical researchers and developers. Moreover, at least 30% of currently marketed drugs also fall into this category (23).

A drug delivery system is considered to have rapid release if at least 85% of the API dissolves within 15 minutes using a rotating basket (USP Apparatus I) (100 rpm, 37±0.5°C) or paddle (USP Apparatus II) (50 rpm, 37±0.5°C) in up to 900 ml of medium, which may include: (a) acidic media, such as 0.1 N HCl or enzyme-free USP Simulated Gastric Fluid (SGF); (b) pH 4.5 buffer; and (c) pH 6.8 buffer or enzyme-free USP Simulated Intestinal Fluid (SIF). If this criterion is not met, the formulation is considered to have slow release (21, 24).

Besides the four BCS classes, it is also important to mention the Developability Classification System (DCS), a modern classification system in the pharmaceutical industry designed to support development of poorly soluble APIs. The DCS focuses on optimizing formulation strategies, recommending key modifications to improve suitability for product development. Biorelevant media were introduced by the DCS creators to provide more reliable assessment of in vivo solubility. Furthermore, BCS Class II was subdivided into two subclasses: DCS II/a. and DCS II/b. Another notable modification was the shifting the dose solubility ratio, resulting in a lower threshold for a molecule to be considered "soluble". DCS II/a. molecules have dissolution rate limitations. Theoretically, if maximum solubility is achieved faster, molecule absorption can be improved. Therefore, development should focus on increasing the dissolution rate. DCS II/b. compounds are so poorly soluble that, regardless of how rapidly the drug enters solution, absorption will not be affected. The fundamental challenge with DCS II/b. molecules is, therefore, solubility (25, 26).

1.3 The development and evolution of dissolution testing

The in vitro assessment of drug release profiles from drug carrier systems is among the critical testing methods in the pharmaceutical industry. In addition to being used for formulation development and quality control of pharmaceutical products, the primary goal of in vitro dissolution measurements is always to predict the in vivo performance of the dosage form. This method has significantly advanced compared to simple disintegration tests, enabling dissolution testing of immediate release (IR) products as an integral part of quality control processes. Research related to dissolution testing began more than a century ago in the field of physical chemistry and has since undergone many significant advancements (27). The first dissolution studies were carried out by Noyes and Whitney in 1897, focusing on the dissolution of benzoic acid and lead-chloride, both known for their poor solubility. These compounds were placed in glass cylinders immersed in water tanks, where the cylinders were rotated at a constant speed and temperature. The authors observed a proportional relationship between the dissolution rate and the difference between the instantaneous concentration c at time t and the saturation solubility c_s, where k is a constant (Equation 1.) (27, 28).

$$\frac{dc}{dt} = k * (c_s - c) \qquad (1)$$

The Nernst-Brunner equation, introduced in 1904, is derived from the diffusion layer model and Fick's second law (Equation 2).

$$\frac{dc}{dt} = \frac{D}{Vh} * (c_s - c) \qquad (2)$$

where $k = D/(Vh)$, D is the diffusion coefficient, h is the thickness of the diffusion layer, and V is the volume of the dissolution medium.

Later, alternative models were available. In 1951, Danckwerts introduced the classic surface renewal model, which provides a quantitative description of gas absorption on the surface of turbulent liquids. This model demonstrates that the gas-liquid interface, where absorption occurs, is continuously refreshed by new liquid elements originating from the bulk (29). In 1961, Higuchi revised the interfacial barrier model and proposed that

interfacial transport, which requires high activation energy, should be considered the rate-limiting step (28).

For tablets, the evolution of disintegration testers and dissolution testers is inseparable. Disintegration testing for tablets was introduced in the Pharmacopeia Helvetica in 1934. The method used water at 37±0.5°C as the medium, applying intermittent agitation (30). Over time, various other disintegration tests were developed, incorporating devices such as tubes and meshes (31), and aimed at reproducing biologically relevant conditions by using simulated gastric fluid as the medium (32). In 1948, Filleborn introduced an artificial stomach model simulating in vivo conditions, including pH, peristalsis, fed state, gastric fluid volume and hydrostatic pressure (33). Despite advances in in vitro dissolution testing, such methods became widely applied only until the early 1950s.

Although numerous physicochemical dissolution experiments were conducted, the first official dissolution tests were adopted by the British Pharmacopoeia in 1945, followed by the USP in 1950 (34). Researchers only began to recognize the importance of dissolution and absorption rates of orally administered drugs in the early 1950s (30). Assuming that a drug is rapidly absorbed from the gastrointestinal tract, the transition of the molecule into dissolved form was identified as the rate-limiting step controlling the appearance of the active ingredient in the bloodstream. This concept was first published by Edwards in 1951 (35), who suggested that if acetylsalicylic acid tablets disintegrate in the stomach, the intestine plays a key role in determining the drug's absorption into the bloodstream (30).

In 1957, Nelson was the first to correlate the in vitro dissolution rate with the blood levels of orally administered theophylline salts (36). However, it was not until the mid-1960s that the impact of the release of the active ingredient from the dosage form and its dissolved state on the therapeutic efficacy of oral drugs became widely recognized. Reports published in 1963 (37) and 1964 (38) highlighted a lack of clinical efficacy. In Canada, two commercially available tolbutamide-containing drug products were found to be less effective than other authorized medicines containing the same active pharmaceutical ingredient. According to studies, this was due to the tablets' slower disintegration and slower active ingredient release (39). Similar results were later found

in studies investigating tablets containing other actives (40). In 1968, Martin and colleagues reported significant differences in the bioavailability of drug products containing diphenylhydantoin, chloramphenicol, and sulfisoxazole among preparations from different manufacturers (41).

The most significant bioavailability problems were reported with phenytoin in the United Kingdom and the United States in 1971, and in Australia and New Zealand in 1968. In the study, a sevenfold difference was observed in serum digoxin levels between products from different manufacturers. This prompted the Food and Drug Administration (FDA) to examine the in vitro drug release profiles of 44 digoxin-containing products from 32 manufacturers. Their results showed substantial differences in the dissolution profiles of the formulations (28, 42). In the case of phenytoin, increased toxicity was observed when lactose was used as an excipient instead of calcium sulfate in a capsule (43). The lower absorption of phenytoin in the original formulation was attributed to the precipitation of insoluble calcium phenytoin salt (44). However, in 1979, Chapron and colleagues found no impact of calcium on phenytoin bioavailability in studies conducted with calcium gluconate. These results suggest that the presence of lactose caused an undesirable increase in plasma concentration, exceeding the narrow therapeutic range (10–20 μg/ml). Chapron concluded that the strong hydrophilic nature of lactose increased the dissolution rate of phenytoin, thus enhancing its bioavailability and resulting in higher plasma concentrations (45).

This period highlighted the critical relationship between solubility and bioavailability. As a result, dissolution tests became an essential tool for quality control. Following these developments, the rotating basket test (USP Apparatus I, designed by M. Pernarowski) was officially accepted as a dissolution tester by the United States Pharmacopeia (USP) and the National Formulary (NF) in 1970 (1, 27, 30, 34, 46). In recent decades, dissolution tests have been standardized, and calibration procedures have also been established.

1.4 Pharmaceutical methods

The evolution of tablet disintegration devices has led to the development of dissolution testers, typically equipped with 6-8 vessels. Alongside test samples, blank or standard samples may also be included. The 11th European Pharmacopoeia (Ph. Eur.) summarizes these most used dissolution tests in its 2.9.3. method (Dissolution tests for solid dosage forms) (47).

1.4.1 USP Apparatus I

USP Apparatus I (rotating basket apparatus) (Figure 2) was first introduced in 1971. In this case, the mixing element is a cylindrical basket. Modern pharmacopeial standards (Ph. Eur., USP, JP) prescribe baskets of standardized size and design made of stainless steel for dissolution testing. Unfortunately, long-term use in acidic or other corrosive media can damage these baskets, which can endanger measured results. To address this, the USP allows a 2.5 μm thick pure gold coating in acidic media or when the drug interacts with the stainless-steel basket. In highly corrosive or solvent-rich conditions, protective coatings such as PTFE (polytetrafluoroethylene), FEP (fluorinated ethylene propylene), and PFA (perfluoroalkoxy alkane) are ideal for protecting the parts. At the beginning of each test, a dose of the test sample is placed into the basket. This method is generally used for measuring capsules, as capsules tend to float to the surface after being dropped into the medium.

1.4.2 USP Apparatus II

USP Apparatus II (paddle apparatus) (Figure 2) was introduced in 1978 (30, 34). These devices are made from stainless steel or other inert materials, and inert surface coatings are also permitted. This method is primarily used to test tablets that sink to the bottom of the vessel before mixing begins. However, for certain dosage forms, such as hard gelatin capsules (48), sticky tablets, or slowly disintegrating tablets, a sinker (Figure 2) is necessary to prevent the sample from floating (34).

Placing the samples in a sinker, such as an 8-mesh basket sinker (Japanese Pharmacopoeia size), spiral capsule, O-ring, or U-type sinker may resolve these concerns allowing the use of the paddle apparatus (49). For floating dosage forms, the United States

Pharmacopeia generally recommends the use of a non-reactive stainless-steel spiral for dissolution testing.

In 1987, various new sinker was defined into four categories by Soltero and colleagues: (a) longitudinal sinkers contact the dosage form along its long axis; (b) lateral sinkers surround the capsule or contact it at the center; (c) cages may be basket-shaped to hold the entire capsule or circular to sit on top of the capsule; (d) internal weights consist of two steel ball bearings (48). These innovations have expanded the applicability of the paddle method for various dosage forms, ensuring accurate and consistent dissolution tests.

Although sinkers can solve floating problems during the dissolution test, their final position in the vessel may vary, thus contributing to device in test results. This variability can be reduced by using a suspended stationary basket, such as the felodipine stationary basket. Nevertheless, reproducibility and accuracy challenges have also been reported with USP Apparatus II.

The primary source of variability is often attributed to the traditional cylindrical vessel, especially the area beneath the rotating paddle. To solve this, newly designed peak vessels have been developed. These vessels effectively eliminate the unmixed formulation cone by directing the API to regions with optimal hydrodynamics. This ensures that the entire product is evenly exposed to the dissolution medium, improving test reliability and reducing variability (50).

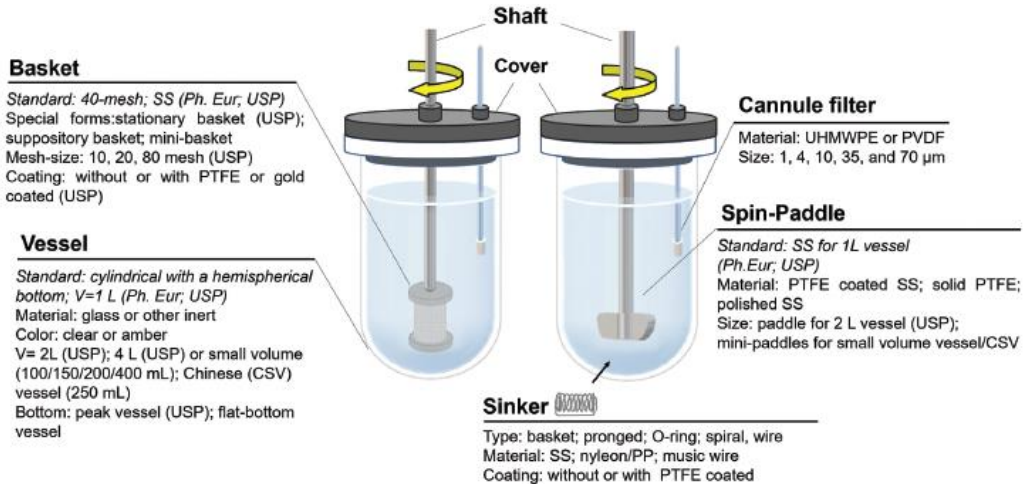

Figure 2 *USP Apparatus I-II and various accessories (own figure, 14) Apparatus I (basket) and Apparatus II (paddle) dissolution devices, along with various types of dissolution vessels, sinkers used to floating samples in place, and cannule filters that help obtain particle-free solution during sampling.*

1.4.3 USP Apparatus III

The vertical reciprocating cylinder method (USP Apparatus III) (Figure 3) was introduced in 1991 (51), designed for testing modified release (MR) formulations, such as sustained release (SR) or delayed release (DR) tablets and capsules. This method is particularly advantageous, as it more efficiently simulates critical physicochemical parameters than USP Apparatus I and II, making it excellent for in vivo predictions (52).

Despite its advantages, the method also has significant disadvantages. It is very labor-intensive and presents challenges for automation, limiting its widespread use and practicality in routine testing environments (27, 51).

Figure 3 *BioDiss dissolution testing equipment (own photo)*

The Biodiss system, a modern dissolution testing apparatus designed for biorelevant media. It enables precise simulation of gastrointestinal conditions, supporting the evaluation of drug release profiles under physiologically relevant environments.

1.4.4 USP Apparatus IV

USP Apparatus IV (flow-through cell device) (Figure 4) was introduced in 1995 as a flow-through method that simulates intestinal peristalsis with pulsatile flow. This innovative design allows for continuous medium exchange and even dynamic pH gradient creation. Researchers can thus examine the effects of pH gradient and continuous removal of the dissolution medium (53).

The device is particularly suitable for testing sustained-release preparations, as it continuously exposes the formulation to fresh medium, modeling absorption in the intestines. Furthermore, USP Apparatus IV has significantly improved in vitro-in vivo correlations (IVIVC) for poorly soluble compounds, making it a valuable device for dissolution testing and formulation development of compounds with poor solubility (54).

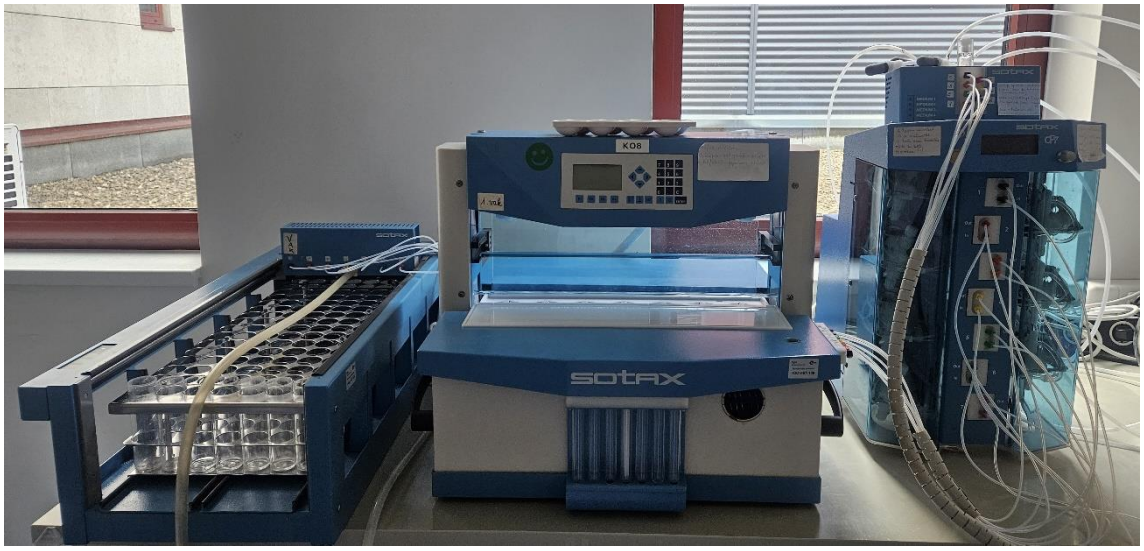

Figure 4 *Flow-through cell dissolution testing equipment (own photo)*

Flow-through cell dissolution testing apparatus, designed for continuous media flow around the dosage form. This system allows precise control of hydrodynamic conditions and is especially suitable for poorly soluble drugs and modified-release formulations.

1.5 European Pharmacopoeial Dissolution Tests

Pharmacopoeia provides varying guidance on conducting dissolution tests. The United States Pharmacopoeia (USP) specifies detailed dissolution methods for many active substances, including the required apparatus, medium, measurement time, and Q value. In contrast, the Ph. Eur. provides only general methodological guidance, leaving the exact parameters to manufacturers and product specifications. For delayed-release solid dosage forms, it describes two approaches. In both methods, the medium must be mixed with the tablets for two hours: (a) in 750 ml or (b) 1000 ml of 0.1 M degassed hydrochloric acid (HCl) at 37±0.5 °C. After this initial phase, the pH can be raised by adding buffer solutions as follows:

(a) By adding 250 ml of 0.02 M trisodium phosphate dodecahydrate solution to the vessel. If necessary, the pH is adjusted to 6.8±0.05 with 2.0 M hydrochloric acid or 2.0 M sodium hydroxide.

(b) After two hours of dissolution in 0.1 M HCl, the hydrochloric media is drained from the vessels and replaced with 1000 mL pH 6.8 phosphate buffer. The buffer solution

is prepared by mixing 0.1 M HCl solution (3 parts) and 0.2 M aqueous solution of trisodium phosphate dodecahydrate (1 part). If necessary, the pH is adjusted to 6.8±0.05 with 2.0 M hydrochloric acid or 2.0 M sodium hydroxide solution.

Alternatively, the entire medium may be replaced by transferring the baskets into a new vessel prefilled with 1000 ml of degassed pH 6.8 buffer solution thermostated at 37±0.5 °C.

In both cases, the solutions are used for a further 45 minutes or as specified. Finally, samples are taken from the solution and analyzed using appropriate qualitative and quantitative methods.

1.5.1 Dissolution medias

Bicarbonate buffers are typically used in vitro to simulate the physiological pH range (5.0 to 8.4) of luminal fluids in the digestive tract. The pH of a bicarbonate buffer is determined by the dynamic interaction of bicarbonate ions (HCO_3^-), carbonic acid (H_2CO_3), dissolved carbon dioxide ($CO_{2(aq)}$), and the partial pressure of CO_2 over the solution (55). Liu and colleagues promoted the development of bicarbonate systems by modifying Hank's buffered saline (pH 7.4) (56), of which pH is too high and buffering capacity too low compared to human intestinal fluids (57). To address this, the buffer was adjusted to create a pH 6.8 bicarbonate solution with increased buffer capacity. Hank's solution primarily acts as a hydrogen carbonate buffer, containing both hydrogen carbonate (HCO_3^-) and carbonic acid (H_2CO_3). The dissociation of carbonic acid contributes to the formation of aqueous carbon dioxide ($CO_{2(aq)}$), ensuring dynamic equilibrium and physiological relevance (58, 59) (Equation 3).

$$CO_{2\,(g)} \rightleftharpoons H_2O + CO_{2\,(aq)} \leftrightarrow H_2CO_3 \leftrightarrow H^+ + HCO_3^- \qquad (3)$$

The pH of the hydrogen carbonate buffer can be set by modifying the concentrations of the acid (H_2CO_3) and its conjugate base (HCO_3^-), as described by the Henderson-Hasselbalch equation (Equation 4):

$$pH = pKa + \frac{HCO_3^-}{H_2CO_3} \qquad (4)$$

Due to the thermodynamic instability of hydrogen carbonate solutions, bicarbonate buffers are less commonly used for dissolution testing of solid preparations (60). The main challenge is the spontaneous loss of CO_2 from the solution, causing irregular increases in pH. To maintain the desired pH, CO_2 loss must either be completely prevented or quantitatively compensated by returning a suitable amount of CO_2 gas to re-establish equilibrium (61).

To overcome these challenges, Al-Gousous and colleagues developed a phosphate-based dissolution method with pH 6.5 phosphate buffer, which produced dissolution profiles similar to those of bicarbonate systems for the tested formulations (62). This approach enables better biological prediction in the fed state. The dissolution behavior of enteric polymers is considerably more complex than that of small molecules; therefore, such innovative approaches are necessary. The molarity of the phosphate buffer has been optimized to similar physiological bicarbonate buffers, making it a practical and reliable alternative (63).

The FDA database for in vitro dissolution testing provides extensive information on various media that can be used for measurements. Alongside simple compositions, complex systems are also available, which may contain surfactants, organic solvents, and enzymes (64). The most frequently used dissolution media listed in the database have pH values ranging from 1.0 to 7.5, with ionic strengths similar to those described in the USP. These pH values correspond to different phases of the gastrointestinal tract (GIT), making them physiologically relevant (64).

Gastric emptying time is influenced by many factors, including nutritional status. In the fasted state, gastric emptying typically occurs within about 30 minutes (65), whereas in the fed state, the process takes longer, averaging about 2 hours. This timeframe can vary significantly across age groups, including healthy adults (20-53 years old) and children 0-5 years (66).

According to the FDA dissolution database, various acidic aqueous solutions can be used as solvents for dissolution testing. The most used acidic media are hydrochloric acid at 0.1 M, 0.01 M, and 0.001 M concentrations, but phosphoric acid (0.01 M) is also widely used (64). For simulating intestinal fluid (SIF), a medium with pH 6.8 is recommended. However, due to its effect on basic test conditions, such as pH and surface tension, water

is not recommended as a dissolution medium. Its low buffer capacity further increases its limitations. Due to interactions between active and inactive components, dissolution conditions may change during the test, complicating the process.

For drugs poorly soluble or insoluble in water, surfactants are often used to increase solubility. Commonly used surfactants include sodium lauryl sulfate (SLS) (4), various polysorbates, lauryl dimethylamine oxide (LDAO), Triton X (67), Brij 35 (polyoxyethylene lauryl ether), and cetyltrimethylammonium bromide (CTAB) (64). However, synthetic surfactants can interfere with the salt formation of weak bases, potentially causing inappropriate effects on dissolution. Sometimes higher pH values may be needed but should remain justified and not exceed pH 8.0. The transit time of formulations in the small intestine is similar in children (68) and healthy adults in the fed state, averaging about 7.5 hours (69). In the fasted state, this time is significantly shorter, approximately 2.5 hours (70).

Although in vivo studies are often limited by ethical considerations, technical challenges, or financial constraints, a deeper understanding of infant digestion provides valuable information. Such knowledge is vital for understanding, for example, how components of infant formula are broken down in the newborn's digestive system. This knowledge is crucial for developing new formulas with enhanced health benefits (55). In recent years there was a little progress in the development of biorelevant media for suitable pediatric dissolution tests (71). Predictive biopharmaceutical methods representing the in vivo drug dissolution in children would be of huge benefit for early formulation screening and influence assessment.

1.5.2 Sampling and detection

Sampling is crucial during dissolution tests. The sampling location in dissolution studies are considered critical as it can significantly affect the accuracy and reproducibility of the results. The position is strictly regulated by pharmacopoeias (e.g., USP, Ph. Eur.). The sampling point is determined by the distance from the vessel wall, the height of the paddle, and the volume of the medium.

Since the media contain insoluble or yet undissolved particles (API or excipients), various filters play an important role in dissolution studies. Filters are typically made

from UHMW PE (ultra-high molecular weight polyethylene), but when chemical compatibility presents a challenge, PVDF (polyvinylidene fluoride) filters may also be used. PVDF shows enhanced chemical resistance and compatibility among thermoplastic materials.

Traditional dissolution testers are often characterized by off-line sampling, where detection does not occur in real time. Samples are collected either manually or automatically and then analyzed away from the dissolution apparatus, sometimes in a different laboratory, typically by UV spectrophotometry or HPLC. The at-line arrangement is faster than the off-line solution; here, sampling and detection occur in the same space. Modern dissolution testing equipment is now designed to facilitate automated sampling, including the removal, filtration, and collection of samples from a defined location at preset intervals. Advanced systems can even measure the concentration of dissolved drug in real time using an integrated spectrophotometer. Many laboratories operate dissolution testers in on-line mode, which allows for automatic sample removal and real-time detection, although even in these cases, the withdrawn sample is physically separated from the process. The collected sample is transported with tubing to an analytical device that detects the dissolved amount of drug substance.

Increasingly, in-line methods are being adopted, in which detection occurs directly within the medium, without removing a portion of the sample. This method enables continuous, real-time monitoring.

Considering its advantages, ICP-OES may be suitable as a process analytical technology (PAT) tool in the pharmaceutical industry, as it can detect changes in chemical composition and, with appropriate tools, can be adapted for real-time monitoring (72).

To guarantee the accuracy of these measurements, rapid detection of the active ingredient concentration and the maintenance of device integrity are essential. Insoluble or undissolved particles, whether active ingredients or excipients, must remain in the dissolution vessel, emphasizing the importance of effective filtration.

1.6 Biorelevant predictive methods

While biorelevant parameters and media enable a more accurate simulation of the gastrointestinal tract, their complexity makes them less suitable for routine in vitro

dissolution studies (73). Biorelevant methods use smaller volumes of fluid (250 ml) for the assay, mimicking the composition of different regions of the digestive system. These include fluids such as fasted state simulated gastric fluid (FaSSGF), fed state simulated gastric fluid (FeSSGF) (Table 1), fasted state simulated intestinal fluid (FaSSIF), and fed state simulated intestinal fluid (FeSSIF) (Table 2) (74-76).

Table 1 *Composition of fasted and fed state simulated gastric fluids*
The table summarizes the compositions of fasted state simulated gastric fluid and fed state simulated gastric fluid.

	FaSSGF	FeSSGF
Pepsin (mg/mL)	0.1	-
Sodium taurocholate (μM)	80	-
Lecithin (μM)	20	-
Sodium chloride (mM)	34.2	237.02
Acetic acid (mM)	-	17.2
Sodium acetate (mM)	-	29.75
Milk:buffer ratio	-	1:1
pH	1.4-2.1	5
Buffer capacity (mmol/l/ΔpH)	41.0±6.0	25
Osmolality (mOsmol/kg)	191±36	400±10
Gastric emptying time (hours)	~0.5	~2.0

Table 2 *Composition of fasted and fed state simulated intestinal fluids*

The table summarizes the compositions of fasted state simulated intestinal fluid and fed state simulated intestinal fluid.

	FaSSIF	FaSSIF-V2	FeSSIF	FeSSIF-V2
Sodium taurocholate (mM)	3	3	15	10
Lecithin (mM)	0.75	0.2	3,75	2
Disodium phosphate (mM)	28.65	-	-	
Maleic acid (mM)	-	19.12	-	55.02
Sodium hydroxide(mM)	8.7	34.8	101	81.65
Sodium chloride (mM)	105.85	68.62	173	125.5
Glyceryl monooleate (mM)	-	-	-	5
Sodium oleate (mM)	-	-	-	0.8
Acetic acid (mM)	-	-	144	
pH	6.5	6.8	5	5.8
Buffer capacity (mmol/l/ΔpH)	12	10	76	25
Osmolality (mOsmol/kg)	270±10	180±10	635±10	390±10
Intestinal transit time (hours)	~2.5		~7.5	

These media not only replicate the composition of human fluids but also include components that ensure buffer capacity and surfactants (such as bile acids and lecithin) at defined pH levels, allowing for a more accurate representation of in vivo dissolution. However, translating the results of dissolution tests into quantitative in vivo performance predictions remains a challenge. Physiological factors such as gastric emptying, intestinal membrane permeability, transit time, and pH can significantly influence bioavailability (77). For oral administration, biorelevant dissolution studies generally focus on three main absorption sites: the stomach, the small intestine, and the colon. The media representing these sites have pH values of 2.0, 6.5, and 6.8, respectively. To ensure homogeneity, the medium should be mixed with stirrers, and the tests are conducted at a temperature between 37±0.5°C. These conditions aim to simulate the physiological

environment, providing a more accurate picture of the drug's in vivo dissolution and absorption.

Methods such as the Artificial Stomach-Duodenum (ASD) simulator offer advanced tools for predicting the behavior of pharmaceutical formulations in the human gastrointestinal tract. The ASD models three key regions: the stomach, the duodenum, and the jejunum (78, 79) (Figure 5). Peristaltic pumps in the system regulate the supply of fluids representing gastric and intestinal secretions, as well as the transfer of contents between the stomach and duodenum and between the duodenum and jejunum.

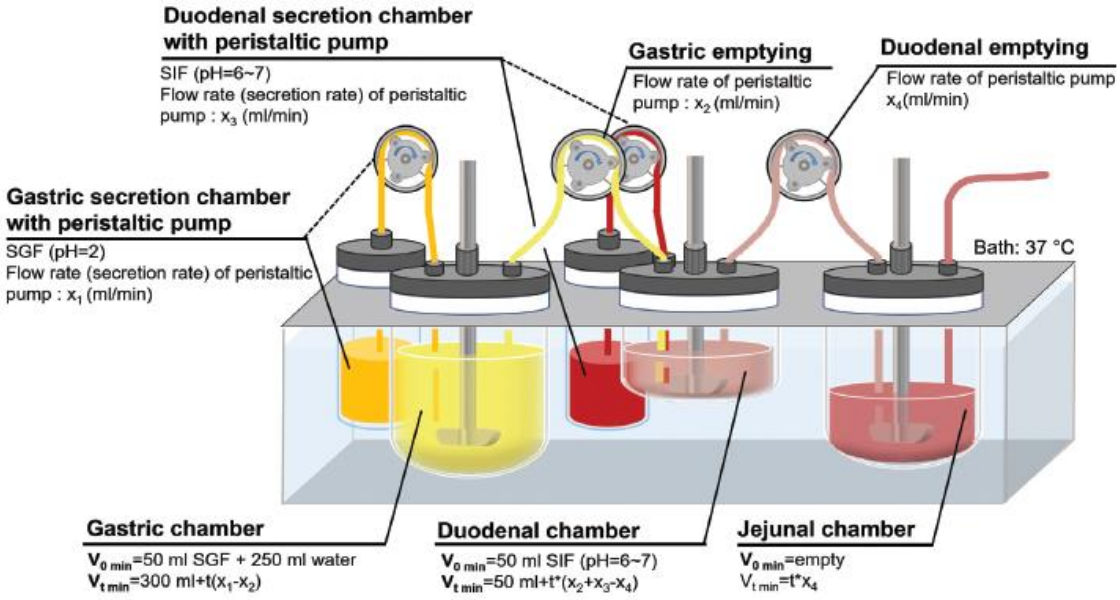

Figure 5 *The GIS dissolution model (own figure, 14)*

The GIS (Gastrointestinal Simulator), a dynamic, multi-compartmental dissolution system that mimics the physiological conditions of the human gastrointestinal tract. It enables advanced in vitro testing of drug release and absorption under biorelevant conditions.

The device enables the optimization of critical parameters, including the speed of the pumps and the temperature of the fluids. Furthermore, the system allows precise pH control, ensuring that conditions closely mimic the dynamic environment of the human

digestive tract. The rotation speed of the stirring paddles is kept constant during measurement by the operators, thus physiological motility is also modeled (80). This simulation device offers a robust platform for evaluating the dissolution and absorption of drugs under conditions that characterize the human digestive system.

1.6.1 Biorelevant medium simulating the stomach

In the fasted state, the simplest dissolution medium is SGF, a pepsin-containing hydrochloric acid solution with a pH of 1.2. Its surface tension is approximately the same as that of water. To reduce surface tension and better physiological conditions, surfactants such as SLS are recommended (4). The pH of the human stomach varies significantly (1.2–6.4) depending on the individual, nutritional status, and the nature of the food consumed. In fasted state, gastric fluid pH typically ranges between 1.2 and 2.7 (81-86). In contrast, in the fed state, the gastric content pH can rise to 3.0–6.4, but the digestive state and food composition have a significant impact (83, 84). This variability highlights the importance of simulating appropriate physiological conditions during dissolution tests.

In 2005, Vertzoni and colleagues introduced FaSSGF, a medium designed to replicate the physiological composition of fasted state gastric fluid based on physiological data. FaSSGF with pH 1.6 contains pepsin, bile salts, and lecithin at physiologically relevant concentrations to achieve in vivo, like surface tension (87).

For fed state simulations, the gastric environment is much more complex than in the fasted state, as its physicochemical properties continuously evolve due to secretion, digestion, and gastric emptying. The initial fed state gastric environment can best be simulated with milk or liquid nutritional products. For these tests, UHT milk (3.5% fat content) is recommended (75, 78-91). FeSSGF consists of a 1:1 mixture of UHT milk and acetate buffer, mixed using a magnetic stirrer and adjusted to pH 5.0 with 0.1 N hydrochloric acid. This medium effectively predicts the effect of food on drug release from the dosage form and can conclude its impact on bioavailability (92). After eating, the gastric pH initially increases due to the buffering capacity of the food and, depending on the composition of the meal, can even reach pH 7.0. Over a few hours, gastric acid secretion gradually returns the pH to basal levels (83, 93, 94).

In 2017, Passannanti and colleagues developed a dynamic in vitro digestive system to mimic infant physiology. This system includes oral, gastric, and small intestinal phases, and serves to evaluate the digestibility of rice starch and rice cream-based baby foods (95). Other studies have used cow's and soy-based infant formulas to simulate the gastric fluid of newborns (96). These advances highlight the accuracy of modeling digestion across different physiological states and age groups.

1.6.2 Biorelevant medium simulating the small intestine

The medium simulating the small intestine (SIF), a pH 6.8 solution containing pancreatin, is the simplest representation of the small intestine. SIF is primarily used for quality control purposes, but is only limitedly applicable for IVIVC, as it cannot reliably predict the effect of food on drug absorption (94). In the human small intestine, the pH gradually increases from the duodenum to the jejunum (2, 69, 97, 98). Changes in pH occur relatively slowly at the beginning of transit (98). In fasted state, the small intestinal pH typically ranges between 6.0 and 7.2. After eating, however, this pH drops to approximately 5.0–6.0, as the food mixes with gastric fluids, which transiently acidifies the neutral environment of the small intestine (73). Upon reaching the colon, the pH decreases further, stabilizing around 5.0 due to the metabolic activity of colonic bacteria and the accumulation of short-chain fatty acids (98-100). This pH gradient is critical for understanding drug dissolution and absorption in different regions of the gastrointestinal tract.

In 1998, Dressman and colleagues introduced a model medium for measurements based on physiological data to simulate the fasted state of the small intestine (4, 75). FaSSIF (pH = 6.5) contains sodium taurocholate and phospholipids in a 4:1 ratio. In 2008, Jantratid and colleagues refined the formulation, resulting in FaSSIF-V2, which has a reduced lecithin concentration (from 0.75 mM to 0.2 mM), lower osmolality, and replaces phosphate buffer with maleate buffer (92).

Using a bicarbonate-based medium in small intestine simulation requires special attention, as CO_2 must be bubbled to maintain stable pH, buffer capacity, ionic strength, and osmolality. To avoid pH instability, phosphate buffers, previously discussed in the earlier thesis section, are often preferred.

For fed state simulations, FeSSIF is used to mimic the small intestinal environment after food intake (4, 75). FeSSIF has a pH of 5.0, with osmolality and buffer capacity adjusted to in vivo conditions. Compared to FaSSIF, FeSSIF contains higher concentrations of sodium taurocholate and phospholipids (101).

Jantratid and colleagues further investigated FeSSIF in studies showing slower pH decline in the jejunum after eating. The updated FeSSIF-V2 includes additional lipolysis products such as glyceryl monooleate and sodium oleate to better reflect postprandial states. FeSSIF-V2 is widely recommended for simulating small intestine diseases (92).

To reflect the effect of digestive processes on the fed-state gastric medium, so-called snapshot media were developed, divided into early, middle, and late phases. These intestinal fluids represent different compositions at specific times after ingestion (92). The simulation of infant and neonatal intestinal fluids, as well as available data on small intestinal transit times, differ significantly from adult values (68, 70).

1.6.3 Biorelevant medium simulating the colon

The colon, although less significant for drug absorption than the small intestine, offers marked advantages when the drug's absorption occurs from this region. These advantages include the long retention time of the dosage form, low enzyme secretion, and direct systemic delivery that bypasses the hepatic first-pass effect. The initial colonic pH varies between 4.8 and 7.0, depending on time and the composition of food intake (102). In 2005, Fotaki and colleagues developed simulated colonic fluid (SCoF – Simulated Colonic Fluid) (Table 3) with a pH 5.8, reflecting physiological pH values and short-chain fatty acid concentrations in the colon (103).

Table 3 *Composition of simulated colonic fluid*

The table summarizes the compositions of simulated colonic fluid.

	SCoF
Acetic acid (mM)	170
Sodium hydroxide (mM)	157
pH	5.8

	SCoF
Ionic strength	0.16
Buffer capacity (mmol/l/ΔpH)	29.1
Osmolality (mOsmol/kg)	295
Transit time (h)	~39

Later, in 2010, Vertzoni and colleagues established simulated media to represent the physicochemical properties of the colon in both fasted and fed states. Fasted state simulated colonic fluid (FaSSCoF) contains tris/maleate buffer solution adjusted to pH 7.8, while fed state simulated colonic fluid (FeSSCoF) uses the same components at varying concentrations, adjusted to pH 6.0. There are significant age-dependent differences in colonic transit times: in children, this is approximately 17.5 hours, in adults 39 hours, and in the elderly (75–80 years) 66 hours (68, 104).

1.7 Gastroretentive Drug Delivery Systems (GRDDS)

Currently, oral administration of solid drug delivery systems remains one of the most widespread and widely accepted methods for delivering active pharmaceutical ingredients (APIs) into the body (105, 106). Solid dosage forms can be highly diverse, such as powders, granules, pellets, microcapsules, microspheres, films (strip), tablets, and capsules. During the release of the drug from the dosage form, it must overcome numerous challenges within the gastrointestinal tract (107). In many cases, conventional oral dosage forms with standard release profiles show limited bioavailability, partly due to rapid gastric emptying time (8). For several active molecules, it is beneficial if the drug remains in the stomach for an extended period. To achieve this, the optimal solution is the design of gastroretentive drug delivery systems (GRDDS), which has been popular in formulation research for several decades. This is particularly advantageous for APIs absorbed in the stomach or the upper part of the intestinal tract, or those that degrade in the intestines (9-11, 108). Over the past decades, various technological approaches (floating systems, expandable systems, magnetic systems, superporous hydrogels, bioadhesive systems, high-density systems) have been developed to prolong the gastric residence time of the delivery system. These solutions can improve the bioavailability of

certain APIs. Another advantage is that the API often releases from the carrier at a pre-designed, slow rate, which helps maintain a more stable blood concentration. As a result, sudden concentration spikes can be avoided, reducing side effects. Due to the prolonged effect, patients need to take their medication less frequently, which improves adherence.

1.7.1 Floating systems

One of the most widely studied forms in this group is the floating drug delivery system, which includes commercially available tablets (e.g., Glucophage XR, Cifran OD, Oflin OD) and capsules (e.g., Madopar HBS floating systems, Valium CR) (109-111). These systems are particularly advantageous for APIs that influence physiological functions of the stomach (for example, antitumor drugs used in gastric cancer treatment) or those with a limited absorption window in the upper gastrointestinal tract (112-114).

Currently, the pharmaceutical industry continues to rely on traditional compression methods to produce floating tablets. The manufacture of gastroretentive floating systems can easily be accomplished by tabletting, using appropriate excipients and optimized compression parameters (115, 116). The widely used tabletting process in the pharmaceutical industry is considered a continuous and cost-effective method (117). The first FDA-approved product (ORKAMBI® (lumacaftor/ivacaftor) from Vertex Pharmaceuticals), produced by a continuous manufacturing process, was also in tablet form (118). There are numerous methods available for characterizing tablets and assessing their compliance with quality requirements, many of which are also included in pharmacopoeias, such as: uniformity of mass testing, uniformity of active ingredient content, friability testing, and crushing strength testing. These tests generally require sampling during the tableting process. Based on a few dozen measurements, predictions can be made about whether the manufacturing process is functioning properly and whether modern rotary tablet presses, which produce thousands of tablets per hour, meet quality standards. However, it is important to note that today's software and hardware capabilities allow for the visual inspection of tablets, from which many properties can be inferred. Imaging is a fast, non-destructive, and cost-effective method that enables the inspection of all units in a production batch (119, 120). It is likely that GRDDS will soon be produced using continuous manufacturing, and in such cases, rapid, non-destructive

techniques like aforementioned VIS imaging-based machine vision will support quality control.

While traditional tabletting technology continues to play a decisive role, several modern manufacturing and formulation approaches, such as 3D printing, offer new possibilities for the development of floating systems. Huanbutta and their team developed a unique system for floatability. They prepared tablet frameworks of various shapes and materials (polyvinyl alcohol, acrylonitrile butadiene styrene, and polylactic acid) using 3D FDM printing. The directly compressed API-containing tablets were placed into a "printlet" containing an air chamber (121).

Low-density gastroretentive systems are drug forms lighter than gastric fluid (approx. 1.004 g/cm³). For this reason, they do not sink but float on the surface of the stomach contents. This floating allows the drug to remain in the stomach longer, providing more time for API absorption. Within this category, there are systems that float due to gas generation and those that float without it (122). Floating systems include gas-generating systems (EFT – Effervescent Floating Tablets) (123), non-gas-generating systems (non-EFT – Non-Effervescent Floating Tablets) (124), and expandable systems. Expandable systems may operate based on swelling (swelling systems) (125) or may mechanically unfold (unfolding systems) (126). In addition to these, bioadhesive systems (127), high-density (sinking) systems (128), superporous hydrogels (129), magnetic systems (130), and ion-exchange resins (131) can also be mentioned, all of which have contributed to prolonging the gastric residence time of tablets.

1.8 Artificial Neural Networks (ANN)

Artificial neural networks are computational models that mimic the functioning of the human brain and are capable of recognizing patterns, classifying data, and making complex decisions. These networks are mathematical models which consist of nodes (neurons) that communicate with each other through weighted connections, and these are simple units of calculation. Neural networks operate through software and implement using programming languages and machine learning libraries. Artificial neural networks are composed of three main layers: the input layer, hidden layers, and the output layer. The input layer receives the data (e.g., molecular features), the hidden layers perform data

processing, and when multiple hidden layers are present, the network is referred to as a deep neural network (DNN). Finally, the output layer provides the network's response, which can be a class label or a real value. The first step in the operation of artificial neural networks is the forward propagation of data through the layers, where each neuron calculates its output. The result from the output layer is then compared to the real value (target variable). To evaluate the network's performance, loss functions are used (e.g., cross-entropy (CE), root mean squared error (RMSE)), which measure how far the network's output deviates from the real value. During training, the errors are backpropagated through the network, updating the weights accordingly. This process enables the network to produce increasingly accurate results. Weight updates are typically performed using gradient-based optimization methods (e.g., scaled conjugate gradient backpropagation) (132, 133). Artificial neural networks can be applied in various areas of the pharmaceutical industry, such as optimizing manufacturing processes. For example, ANNs can be used to model the mechanical properties of tablet compression, allowing prediction of the final product's quality, or in the case of floating tablets, to predict floating behavior (120). Additionally, they can be used for identifying and optimizing drug candidates, pharmacokinetic and pharmacodynamic modeling, analyzing clinical trial data, and more. However, a major challenge is the need for large amounts of reliable data for training.

2 Objectives

During my research, my first goal was to analyze the effects of different dissolution media, considering their role in the dynamics of drug release.

Following this, I focused on the significance of gastroretentive floating drug formulations. The floating ability and its changes over time were monitored during the in vitro dissolution testing of caffeine-containing floating tablets, providing an opportunity to explore the relationship between dissolution and floating properties. For this, I aimed to prepare tablets with identical compositions using direct compression at different compression forces, intending to determine how tablet hardness influences floating behavior and the speed of dissolution. To support this, I calculated the density of the tablets based on their physical parameters (shape, height, mass). During the work, microscopic images were taken of the tablet surfaces, with the aim of correlating surface brightness with the hardness of the formulation. The main objective of the investigation was to be able to predict the floating behavior and dissolution profile of the tablets based on their physical parameters, as well as using a microscopic image of the formulation. This method provides a fast, non-destructive procedure suitable for quality control of floating tablets during changes in the manufacturing process. Subsequently, the various compressed samples were classified using machine vision based on VIS imaging, employing a neural network-based program. The samples were categorized both by their surface properties and their floating characteristics.

In the continuation of my work, I aimed to investigate the applicability of ICP-OES combined with an in vitro dissolution testing apparatus. In this experiment, ibuprofen sodium pellets were used as a model compound with the purpose of simultaneously determining, in-line, the salt concentration of the active ingredient and the drug's dissolution profile. Later, the pellets were filled into straws to simulate an innovative method of administration.

3 Methods

3.1 Materials

3.1.1 Materials used for testing floating tablets

Caffeine (Molar Chemicals, Budapest, Hungary) was used as the model active ingredient. Kollidon® SR from BASF SE (Ludwigshafen, Germany) was applied as a tableting excipient. Isomalt, an official excipient in pharmacopoeias (European Pharmacopoeia, United States Pharmacopeia), is a water-soluble filler suitable for direct compression, facilitating improved tablet ability and loosening the polymer matrix in water. It was supplied by the manufacturer (BENEO-Palatinit GmbH, Offstein, Germany) in agglomerated spherical particle form (galenIQ™ 721). Magnesium stearate was sourced from Molar Chemicals (Budapest, Hungary). Purified water used for measurements (18.2 MΩ cm, 25 °C) came from an ELGA PURELAB Ultra water purification system. Standard solutions and the buffer were prepared in volumetric flasks marked "A." For the pH 1.2 medium, hydrogen chloride (HCl) (Molar Chemicals Ltd.) was used.

The 330 mg (adjusted mass) tablets contained 24.50% w/w caffeine as the model active ingredient. In addition to the active ingredient, the formulation included the following excipients: 62.50% w/w Kollidon® SR polymer as a matrix retarding agent, 12.00% w/w isomalt as a water-soluble filler, and 1,00% w/w Mg-stearate as a lubricant. A laboratory-scale V-blender (Xinxiang Chenwei Machinery Co., Ltd.; China) was used to prepare a 300 g homogeneous powder mixture. Homogenization was carried out at 40 rpm for 30 minutes under the specified parameters. The homogeneous tableting premix was directly compressed using an eccentric tableting machine at six different compression forces (Fette Exacta 1, Fette Compacting GmbH, Schwarzenbek, Germany). Round, flat, without break line tablets with a diameter of 10 mm and an average mass of 330 mg were produced.

3.1.2 Use of medicated straws for simulation studies

Pellets containing ibuprofen sodium (Sigma Aldrich; India) were used as the model compound. Subsequently, the straws were prepared as an innovative dosage form using pellets. The pharmacopoeia does not provide specific methods for testing pharmaceutical

straws; however, several research groups have studied these dosage forms (134, 135). Precisely weighed 1000 mg of pellets were filled into transparent PP-based straws (19 cm high, 0.9 cm diameter; VitaSip Ltd., Hungary) and sealed with a custom-made straw-sealing machine.

3.2. Methods

3.2.1 Investigation of gastroretentive dosage forms

Uniformity of mass

The mass uniformity of the manufactured caffeine tablets was determined by weighing 20 tablets on an analytical balance (Kern ABJ-NM/ABS-N, Kern&Sohn GmbH, Germany). The uncoated tablets weighed 330 mg, and according to pharmacopoeial requirements, no more than 2 out of the 20 individually weighed tablets may deviate from the average weight by more than ± 5%, and none may deviate more than ± 10% (136).

Crushing strength

The resistance to crushing (N) of the tablets was determined using an Erweka breaking force measuring device (Erweka GmbH, Germany). Ten tablets were tested, and results were presented as the average and corresponding standard deviations.

Friability

Friability was assessed with an Erweka friability tester (Offenbach/Main, Germany). During the test, the drum was rotated at a speed of 25 rpm for 4 minutes with 20 tablets. The weight of the tablets was measured before and after the test, dust-free, on an analytical balance (Kern ABJ-NM/ABS-N, Kern&Sohn GmbH, Germany). According to the pharmacopoeial requirements, the maximum weight loss during the friability test should not exceed 1% (137).

High and calculated density of tablets

Tablet heights (thickness) were analyzed using images taken with a digital microscope (Keyence VHX-970F; Keyence Corp., Osaka, Japan), with analysis performed using ImageJ software (Wayne Rasband, National Institute of Health, USA).

Considering the tablet height, shape (round, flat, diameter: 10 mm), and weight, the tablet densities were determined according to the 5th equation:

$$\rho = \frac{m\,(g)}{V\,(cm^3)} \tag{5}$$

where *m* is tablet weight and *V* is the tablet volume.

To calculate the volume of the tablets (Equation 6), I used the radius *r* and height *h* of the tablets:

$$V = r^2 * \pi * h \tag{6}$$

Content uniformity

To determine content uniformity, 10 dosage units were individually measured in all cases. Each of the 10 tablets were placed in a 100 ml flask, filled with solvent (purified water adjusted to pH 1,2 using cc. HCl) and stirred for 60 minutes with a magnetic stirrer at 600 rpm. It was then homogenized and centrifuged at 4000 rpm for 10 minutes. Mixing was performed with a MIX 15 eco 2 core magnetic stirrer, and centrifugation with a Thermo Science Megafuge 16 centrifuge. Finally, each sample was diluted with the solvent to a concentration of 100 µg/ml. Solutions were detected at 273 nm with a Thermo Scientific UV spectrophotometer.

In vitro dissolution test

The dissolution test—according to the 11th European Pharmacopoeia, method 2.9.3 (Dissolution test for solid dosage forms)—was performed using a paddle apparatus (Varian VK 7025 type), with offline UV spectrophotometry (Mettler Toledo UV7, serial no.: B951794301) (47). The dissolution method parameters were: 900 ml pH 1.2 HCl (degassed purified water adjusted to pH 1.2 using cc. HCl), 75 rpm, normal vessel, 10 µm sampling filter. The volume of collected sample was 2 ml. The medium temperature was 37.0 ± 0.5 °C. Sampling times were 15, 30, 60, 90, 120, 240, and 360 minutes. After sampling, the samples were diluted with the medium to a concentration of 100 µg/ml. Detection was performed in a 10 mm cuvette at 273 nm. The dissolution test was performed on three parallel samples.

Evaluation of floatability by machine vision

During the dissolution test, images were taken at the sampling points with an Olympus OM-D E-M10 Mark II camera (Olympus Corp., Tokyo, Japan). The camera position remained unchanged throughout the experiments. Image processing and analysis were performed using MATLAB R2020a software (MathWorks, Natick, MA, USA). After importing the images, the next step was background removal to define the regions containing the dissolution vessel. Afterwards, binarization was performed using the B (blue) component. In the next step of preprocessing, the stirrer also had to be removed from the binary image to prevent interference with the program's recognition. This was followed by selecting the sample using a bounding box. Before measurements, the length of the dissolution vessel in pixels was determined using the images taken. The vertical position of the sample in the vessel at each sampling point was then calculated as a percentage.

Microscopic imaging

The setup for imaging was previously published by Mészáros et al. (119). A Canon 650D DSLR camera and a Canon EFS 18–55 mm objective (Canon Inc., Tokyo, Japan) was used. The objective was to be attached to the camera body with a reversing ring. The camera was connected to a laptop with a USB 3.0 interface. For imaging, illumination was provided by a ring lamp equipped with three rows of light-emitting diodes (Apokromát Kft, Budapest, Hungary). To eliminate ambient light intrusion, imaging was performed in a black box. With this arrangement, both sides of the samples could be examined, resulting in a total of 360 images.

Classification of samples using VIS imaging-based machine vision

Image processing and analysis were performed with MATLAB R2020a software (MathWorks, Natick, MA, USA). The Wavelet Toolbox 5.4 (MathWorks, Natick, MA, USA) enabled multivariate wavelet texture analysis (MWTA) on the samples. Classification relied on pattern recognition neural networks using the Deep Learning Toolbox 14.0 (MathWorks, Natick, MA, USA). The K-nearest neighbor classification method was implemented using Statistics and Machine Learning Toolbox 11.7.

Imported images were resized by 50% to optimize algorithm runtime. Images were binarized on the R (red) component, and Hough transformation was used to identify the required area (the sample) and remove the background. This was followed by enhancing contrast and brightness to highlight surface structuring.

Further steps required the use of the G (green) component and two types of wavelets. MWTA enabled examination of the tablet surface and the creation of the input dataset for classification based on crushing strength and floatability. By using MWTA, the applied wavelet processes the image as a signal and generates scaled and shifted versions of the original wavelet (119). Single-level wavelet decomposition was carried out in two steps. Initially, the Daubechies2 wavelet was applied, followed by a second and third sequential decomposition using Meyer filters. Then, histograms were generated from the resulting approximation coefficients.

To optimize the pattern recognition neural networks, the number of neurons in the hidden layer was adjusted between 1 and 10. The softmax transfer function was applied in the output layer and scaled conjugate gradient backpropagation enabled the measurement during training. The end of the training process was determined by reaching the preset number of validation checks. For each tablet produced at different compression forces, 70% of the samples constituted the training set, 15% validation, and 15% test set. The classes were assigned in a target matrix according to the measured values of crushing strength or floatability. Network performance was evaluated by cross-entropy and root mean squared error, with confusion matrixes also being significant. Samples could also be classified based on their floatability using the height. For this task, a K-nearest neighbors classifier method was important, applying Euclidean distance to classify samples into three classes. For this, data were split so that 70% of the samples were assigned to the training set, and 30% to the test set.

3.2.2 Application of ICP-Oes in in vitro dissolution test

The dissolution profile of ibuprofen sodium pellets was examined using a Hanson Vision Elite 8 apparatus (Hanson Research, USA) with the paddle method. The test was conducted in 900 ml of purified water at 37 ± 0.5 °C. Additional dissolution parameters: 75 rpm, normal vessel. The concentration of the released active ingredient was

determined with an in situ Pion Rainbow fiber optic spectrophotometer (Pion Inc., USA) equipped with a head fitted with a 5 mm probe. Absorbance was detected at 273 nm (138) (Figure 6).

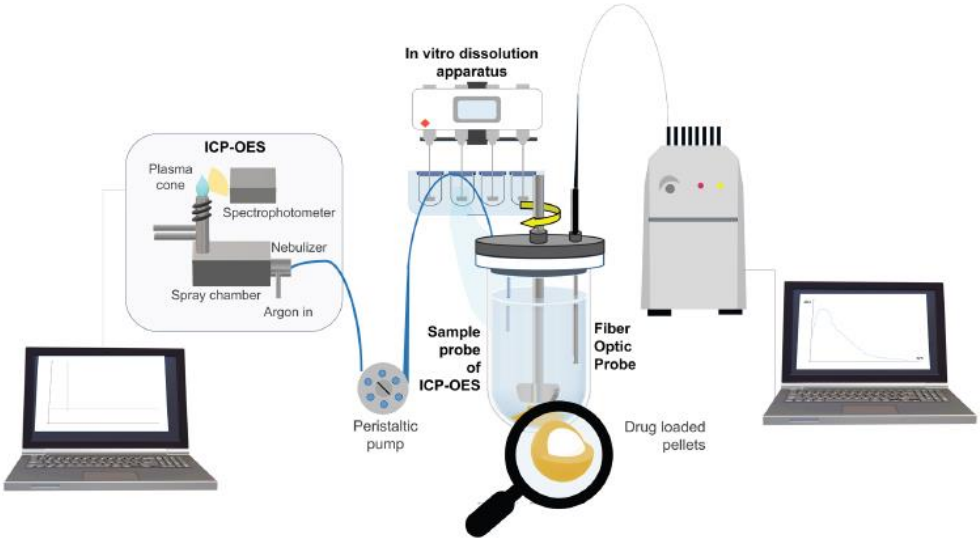

Figure 6 *Dissolution testing of ibuprofen sodium pellets and determination of sodium concentration (own figure, 72)*

The image shows a connected system designed to illustrate the simultaneous application of ICP-OES and Apparatus II dissolution testing, where ibuprofen sodium is dissolved and both the sodium salt concentration and the active ingredient content are measured at the same time.

To determine the sodium concentration, a Spectro Genesis inductively coupled plasma optical emission spectrometer (ICP-OES) (Spectro Anal. Ins. GmbH; Germany) was used with the parameters listed in Table 4.

Table 4 *ICP-OES setup parameters (72)*

The table summarizes the parameters and the settings of the ICP-OES which were used for the measurement.

Parameters	***Settings***
Radio frequency power	1350 W
Auxiliary Ar flow rate	0.80 l/min
Pneumatic nebulizer Ar flow rate	0.85 l/min
Pump speed	2 Step
Wavelengths	589.59 nm
Coolant flow	0.80 l/min
Light tube	0.90 l/min
Optic flush	1.00 l/min
Optic temperature	29.91 °C (29.0 - 31.0 °C)
Osc. exhaust	222.2 Imp/s (min 170.0)
Osc. impedance	5875 Ohms
HVPS current	583 mA
HVPS voltage	3425 V
Flow optic flush	1.00 L/min
Flow light tube	0.90 L/min (0.8 - 1.8)
Nebulizer pressure	2.48 bar (2.0 - 4.0)
Main Ar pressure	7.01 bar (6.0 - 8.0)

To simulate oral administration, a medicated straw was used, which was placed in 250 ml of purified water. The liquid was drawn through the straw by a peristaltic pump (Locost Kft., Tiszaalpár, Hungary) into 250 ml of hydrochloric acid medium (pH 1.2 (degassed purified water adjusted to pH 1.2 using cc. HCl); 37±0.5 °C) at a pump flow rate of 15.6 Hz for 5 minutes to mimic gastric conditions. The concentration of ibuprofen and sodium was determined using the same instruments and settings as those employed for the analysis of pellet release in this medium (Figure 7).

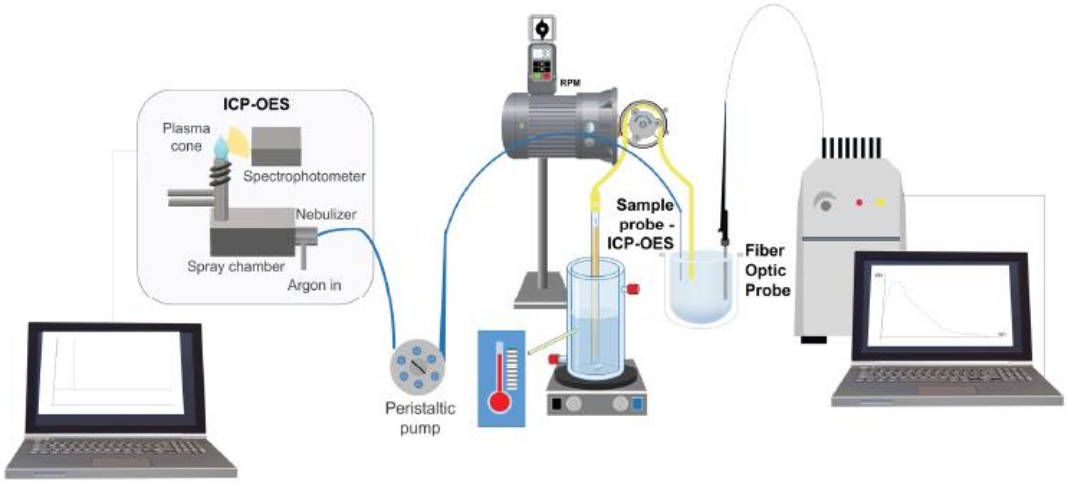

Figure 7 *Simulation of liquid administration through a medicated straw. (own figure, 72)*

The image simulates a new drug administration method using a pump to circulate the medium through a medicated straw. The aim is to simultaneously determine the salt concentration with ICP-OES and the active ingredient content.

4 Results

4.1 In vitro dissolution and floatability of the floating tablets

4.1.1 Physical properties and content uniformity of the tablets

For the study, caffeine-containing gastroretentive floating tablets were prepared by direct compression (DC) using six different compression forces (10N=T/I, 30N=T/II, 45N=T/III, 75N=T/IV, 100N=T/V, 170N=T/VI). The tablet formulations contained significant amounts of direct compression excipients (Kollidon® SR and galenIQ™ 721), which have been successfully used in direct compression according to several previous publications (139, 140). According to the method of the 11th European Pharmacopoeia 2.9.5. (141), the tablets complied, as their average individual weight (n = 20) fell within the acceptable range (313.50–346.50 mg). As expected, increasing the compression force during production improved the mechanical properties of the tablets. Harder tablets exhibited higher crushing strength, and except for T/I and T/II, all met the requirements of the European Pharmacopoeia (2.9.7.), being characterized by friability values below 1% (137). The magnitude of the applied compression force also influenced the density of the tablets. Table 5 clearly shows that as the compression force increased, so did the density of the tablets.

Table 5 *Physical properties of the tablets (mean ± SD, n.a: not acceptable) (120).*
The table summarizes the individual mass (mg), tensile strength (N), friability (%), tablet height (mm), density (g/cm^3) and drug content of the tablets with different crushing strength.

	Individual mass (mg)	**Tensile strength (N)**	**Friability (%)**	**Tablet height (mm)**	**Density (g/cm^3)**	**Drug content (%)**
T/I.	335.7 ± 2.2	13.0 ± 2.5	n.a. (6.53)	4.93	0.87	90.4 ± 1.3
T/II.	328.8 ± 1.6	44.5 ± 3.2	n.a. (1.20)	4.42	0.95	89.9 ± 1.7
T/III.	333.6 ± 1.8	65.2 ± 3.5	0.88	4.25	1.00	89.7 ± 1.1
T/IV.	333.5 ± 2.6	95.0 ± 6.6	0.52	4.02	1.06	89.5 ± 0.9

	Individual mass (mg)	Tensile strength (N)	Friability (%)	Tablet height (mm)	Density (g/cm^3)	Drug content (%)
T/V.	331.0 ± 2.0	127.3 ± 9.7	0.17	3.91	1.08	87.1 ± 1.7
T/VI.	337.0 ± 6.6	204.0 ± 13.6	0.03	3.70	1.16	92.9 ± 3.9

The tablets produced with the lowest compression force had a density of 0.87 g/cm^3, while those made with the highest compression force had a density of 1.16 g/cm^3. Previous publications indicate that the buoyancy threshold for tablets is around 1 g/cm^3 (8). Of my model tablets, 3 samples (T/IV., T/V., T/VI.) were outside this threshold.

According to the results of the caffeine content determination, the active ingredient content was satisfactory in all cases among the tablets compressed with different forces. The content uniformity for the different strength tablets I measured was 87.1–92.9%, summarized in Table 5. The results show that the tableting premix was homogeneous and all test samples complied with the pharmacopoeial requirements for content uniformity (136).

4.1.2 In vitro drug release and determination of floatability by machine vision

As a matrix-forming excipient, Kollidon® SR was used for preparing the gastroretentive floating tablets, consisting of approximately 450,000 molecular weight, 80% water-insoluble poly(vinyl acetate) and 19% water-soluble poly(vinyl pyrrolidone). This excipient has also been used successfully in floating tablet formulations in several previous publications (142-145). According to Figure 8, it can be observed that the release of the active ingredient from the floating system did not occur 100% in all cases. The release of the active ingredient from the tablets with higher compression force occurred at a slower rate. This is demonstrated by the fact that with the highest compression force (170N), about 40% of the active substance was released in six hours, while with the lowest compression force (10N), about 80% dissolved at the same time. It was also observed during dissolution that the tablets swelled upon contact with the medium.

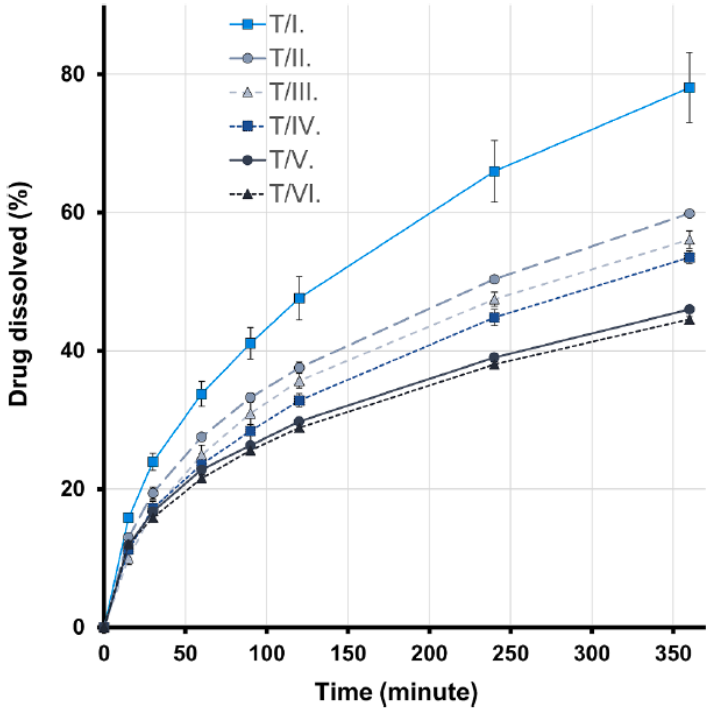

Figure 8 *Dissolution profiles of tablets produced with various compression forces (mean ± SD; n=3) (own figure, 120)*

The image shows dissolution profiles of six tablets prepared with different compression forces (T/I.=10N, T/II.=30N, T/III.=45N, T/IV.=75N, T/V.=100N, T/VI.=170N). The dissolution rates vary according to their floatability, with more floatable tablets exhibiting faster drug release.

During the in vitro drug release study, I recorded the position of the tablets in the floating systems using a camera. With the help of the recorded images, I determined the position of the tablets in the medium using machine vision. Figure 9 illustrates the captured images and the machine vision process, showing the tablets' positions in the dissolution medium. The results of the image analysis related to floating properties are summarized in Table 6.

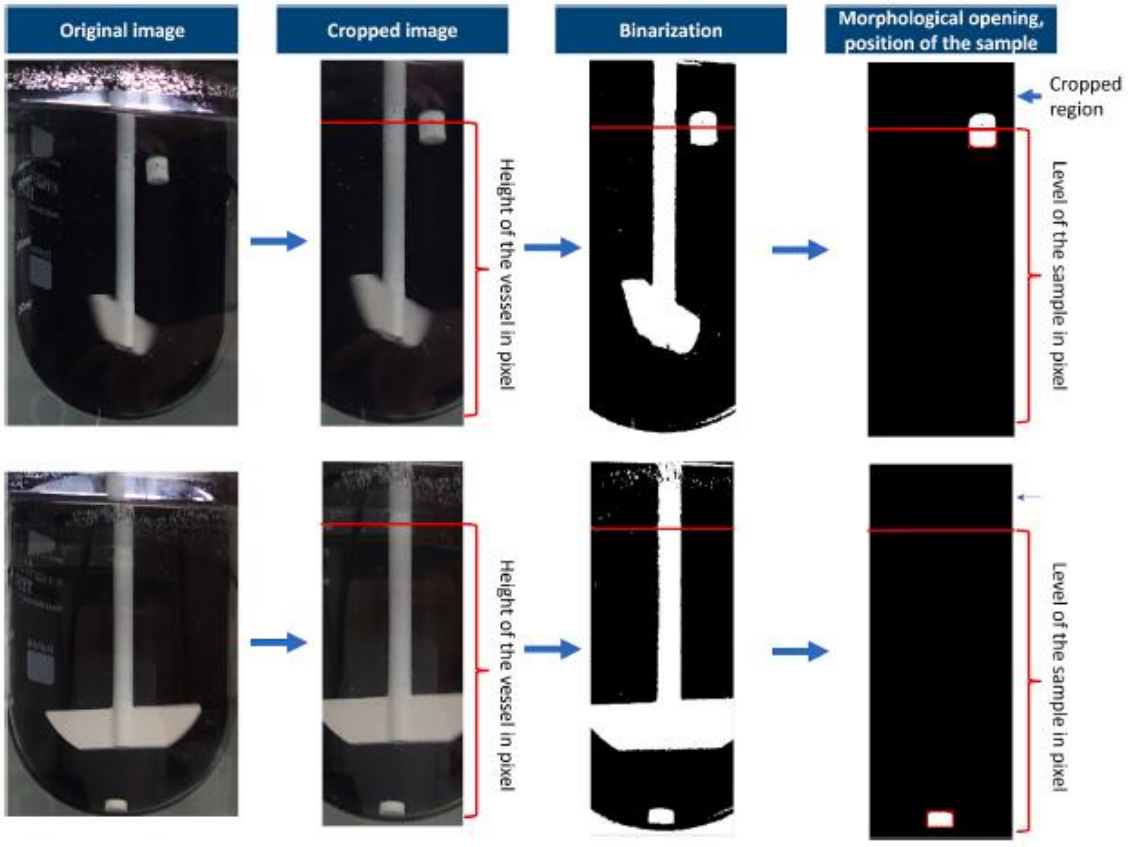

Figure 9 *Assessment of floating by machine vision (own figure, 120).*

The image illustrates the evaluation of tablet flotation using machine vision technology. The analysis is based on an original image, which helps to determine the position of the tablet in the dissolution medium, allowing for real-time evaluation of the flotation behavior.

Table 6 *Floating capacity of the prepared tablets (%; mean ± SD) (14)*
The tablet summarizes the different floating capacity of the tablets with different crushing strengths for 360 minutes.

Time (minute)	T/I.	T/II.	T/III.	T/IV.	T/V.	T/VI.
0	98.1 ± 1.1	95.0 ± 1.5	94.4 ± 0.8	8.1 ± 1.6	9.4 ± 2.4	5.0 ± 0.7
15	98.7 ± 2.0	96.0 ± 0.7	95.3 ± 2.8	9.6 ± 0.8	16.9 ± 7.1	6.2 ± 1.7
30	96.8 ± 1.2	94.9 ± 0.7	94.6 ± 1.5	11.2 ± 1.4	14.5 ± 4.9	4.8 ± 0.2
60	98.5 ± 1.1	95.3 ± 1.2	93.0 ± 0.8	17.1 ± 8.0	67.2 ± 27.3	5.9 ± 1.5
120	98.2 ± 0.8	98.0 ± 0.7	97.8 ± 2.5	34.8 ± 25.7	86.4 ± 12.8	5.7 ± 1.0
240	98.1 ± 0.9	95.7 ± 0.6	94.9 ± 1.9	90.4 ± 5.2	92.1 ± 4.3	10.5 ± 0.7
360	99.3 ± 0.6	98.0 ± 0.4	96.6 ± 2.8	96.4 ± 3.5	97.0 ± 2.7	10.4 ± 0.7

The results show that tablets prepared with low compression force (T/I, T/II, and T/III) remained in the upper region of the medium throughout almost the entire duration of the test. In contrast, the T/IV tablet, produced with higher compression force, showed movement during the first hour of the active ingredient dissolution study, floated in the medium, and then surfaced at the 6th hour. T/V behaved similarly to T/IV, while the T/VI tablet, manufactured with the highest compression force, remained practically stationary at the bottom of the vessel during the dissolution test.

Images of the sample surfaces produced with different crushing strengths are shown in Figure 10. Regions of varying shades appear on the surface, resulting from the different components in the sample compositions. However, these factors did not influence the classification of the samples. This was caused by the combination of caffeine as the active ingredient and specific excipients. Slight differences in surface texture appeared from 10N to 45N and from 75N to 170N. Subtle differences, visible even to the naked eye, can be observed among the samples shown in Figure 10. Analysis of surface texture, as applied in earlier publications by Mészáros et al., allows for the detection of the crushing strength and compression force of the samples. As a result, the

evaluation of compression dependent parameters can be indirectly performed by analyzing surface texture using VIS images (135). Consequently, the machine vision-based approach may be suitable for assessing the floatability of the samples. Based on the observations mentioned, the classification of these samples can still be challenging.

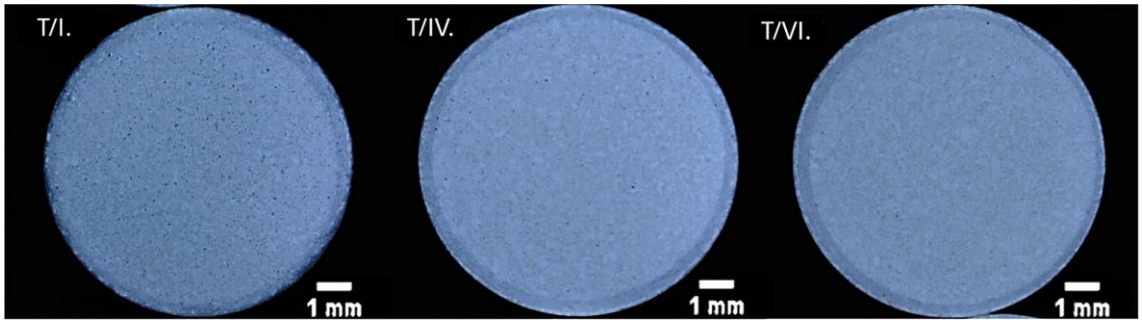

Figure 10 *VIS images recorded of T/I, T/IV, and T/VI samples (120)*
VIS images recorded of T/I, T/IV, and T/VI samples, showing visual differences in tablet surface and structure. These images support the evaluation of formulation characteristics and potential correlations with dissolution behavior.

4.1.3. Classification based on crushing strength and floatability

Image processing algorithms and neural networks were used to classify the samples according to their crushing strength and floatability. The input dataset was created solely from the captured images. By using the measured crushing strength values, the target classes could be defined, resulting in six applied classes. The classification task became complicated due to the large number of groups and minimal surface differences. The summary of the test set's cross-entropy (CE) and relative mean squared error (RMSE) values during the optimization process is presented in Figure 11. The various confusion matrixes obtained are shown in Figure 12.

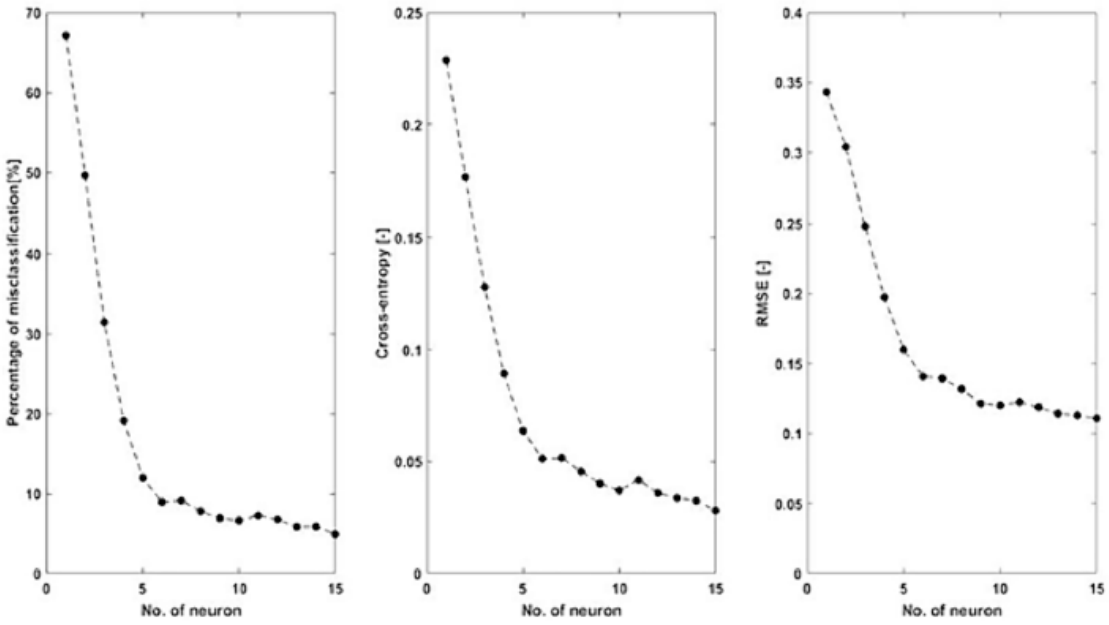

Figure 11 *The obtained average error (%), cross-entropy, and test set RMSE throughout the entire optimization process for classification based on crushing strength (120)*

The image presents the obtained averaged error (%), cross-entropy, and test set RMSE throughout the entire optimization process for classification based on tablet crushing strength. The visualization highlights how the model converges over time and how well it distinguishes between different compression levels, supporting the development of robust classification algorithms for pharmaceutical applications.

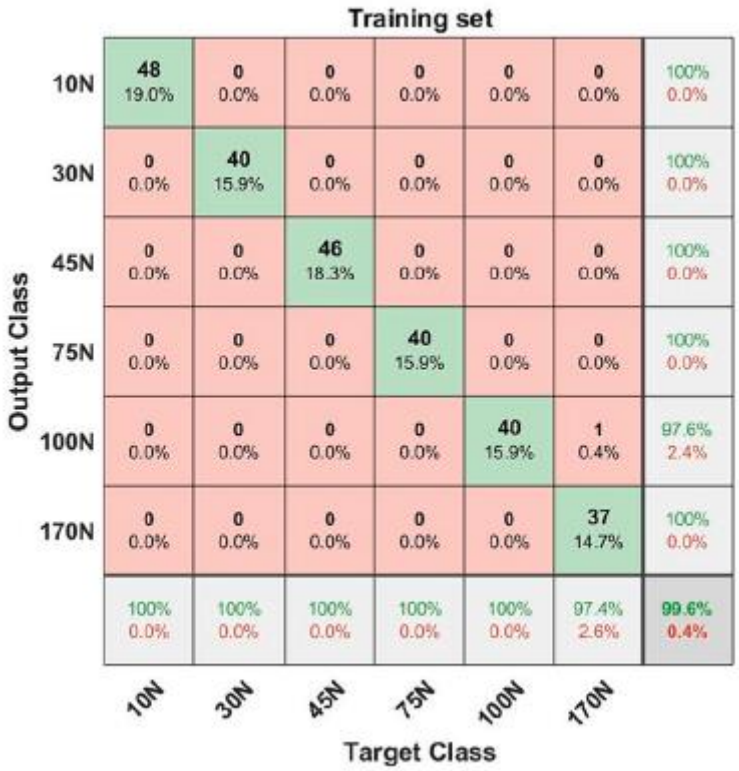
Training set
10N
30N
45N
75N
100N
170N
Output Class
48 19.0%
40 15.9%
46 18.3%
40 15.9%
40 15.9%
37 14.7%
1 0.4%
100% 0.0%
97.4% 2.6%
99.6% 0.4%
Target Class

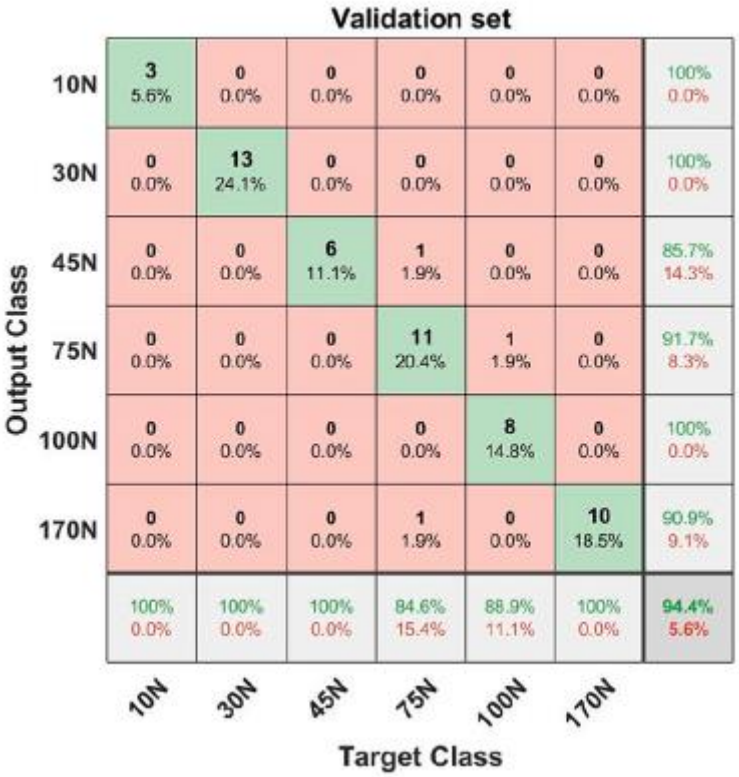
Validation set
10N
30N
45N
75N
100N
170N
Output Class
3 5.6%
13 24.1%
6 11.1%
1 1.9%
11 20.4%
1 1.9%
8 14.8%
10 18.5%
100% 0.0%
85.7% 14.3%
91.7% 8.3%
90.9% 9.1%
84.6% 15.4%
88.9% 11.1%
94.4% 5.6%
Target Class

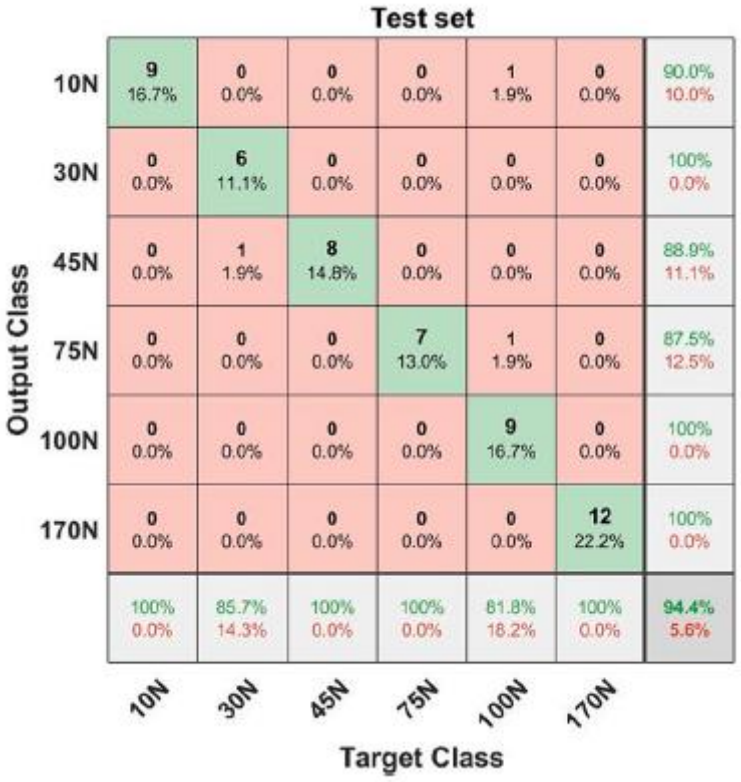

Figure 12 *The obtained training, validation, and test matrixes for classification based on crushing strength (120)*

The image shows the obtained training, validation, and test matrices used for classification based on tablet crushing strength. These datasets form the foundation of the machine learning workflow, enabling model training, performance evaluation, and generalization assessment across different compression levels.

Considering the percentage of samples classified into incorrect categories as well as the CE and RMSE values, the dataset generated from the images can be used to train a Probabilistic Recurrent Neural Network (PRNN). In the hidden layer, 15 neurons were selected, which resulted in low CE and RMSE values. According to the confusion matrixes, only 1 sample from the training set and 3-3 samples from the validation and test sets were misclassified. The aforementioned 7 misclassified samples accounted for roughly 2% of the total dataset. The proportion of misclassified samples in the test set was about 6%. The results indicate that machine vision based on the visible spectrum,

combined with pattern recognition neural networks, can be used to classify these samples according to crushing strength.

The machine vision system is also potentially capable of classifying the floatability of the prepared samples based on the goodness parameters mentioned. After optimization, the PRNN's hidden layer consisted of 13 neurons (Figure 13). In the matrixes (Figure 14), it was established that only two samples in the test set were assigned to incorrect categories, which resulted in a 0.6% error rate for the entire dataset. Within the test set, the proportion of misclassified samples was about 3%. Based on these results, VIS-based machine vision combined with pattern recognition neural networks can be utilized for classifying these samples according to their floating properties.

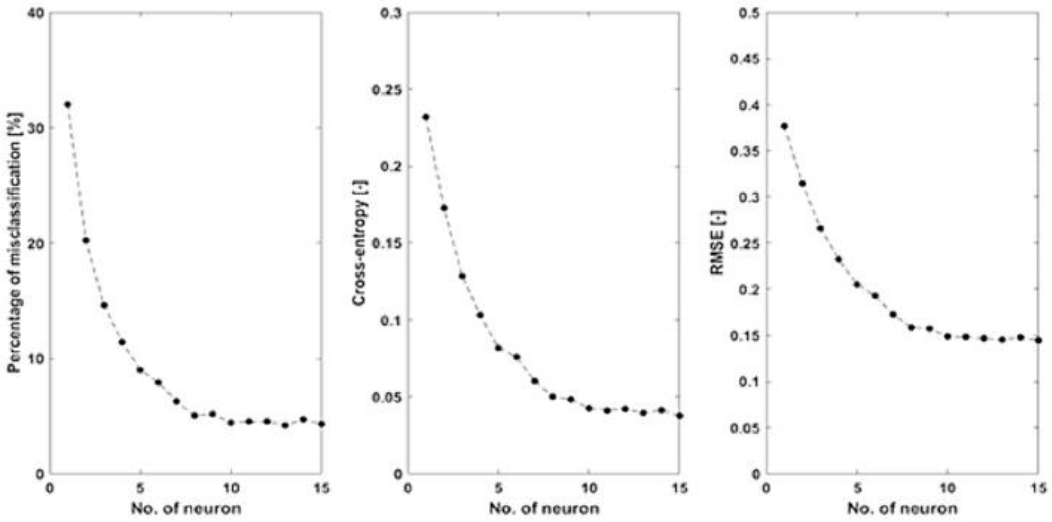

Figure 13 *The obtained average error (%), cross-entropy, and test set RMSE throughout the entire optimization process for classification based on floatability (120) The image presents the obtained average error (%), cross-entropy, and test set RMSE throughout the optimization process for classification based on tablet floatability. These metrics provide insight into the model's learning dynamics and its ability to accurately distinguish between different floating behaviors, supporting the development of predictive tools for formulation performance.*

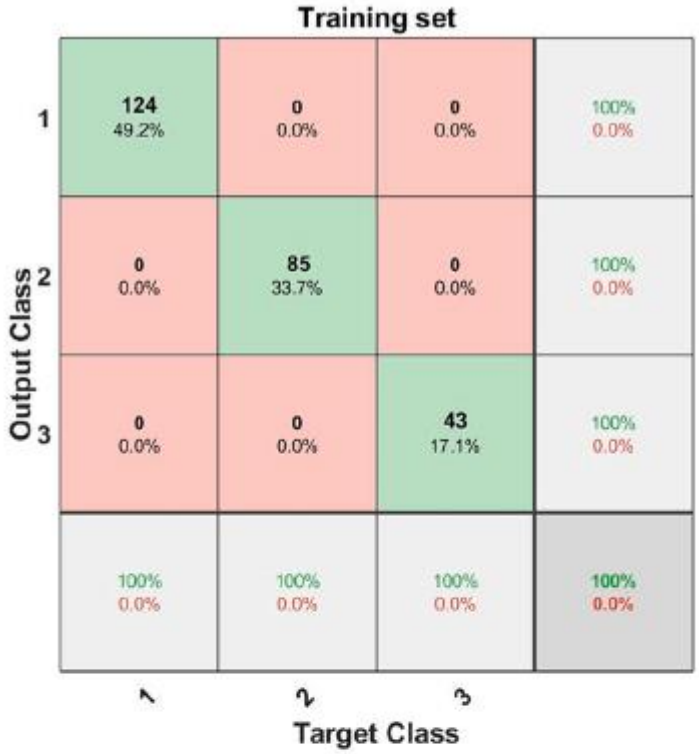
Training set
124
49.2%
0
0.0%
0
0.0%
100%
0.0%
0
0.0%
85
33.7%
0
0.0%
100%
0.0%
0
0.0%
0
0.0%
43
17.1%
100%
0.0%
100%
0.0%
100%
0.0%
100%
0.0%
100%
0.0%
100%
0.0%
100%
0.0%
Output Class
1
2
3
Target Class
1
2
3

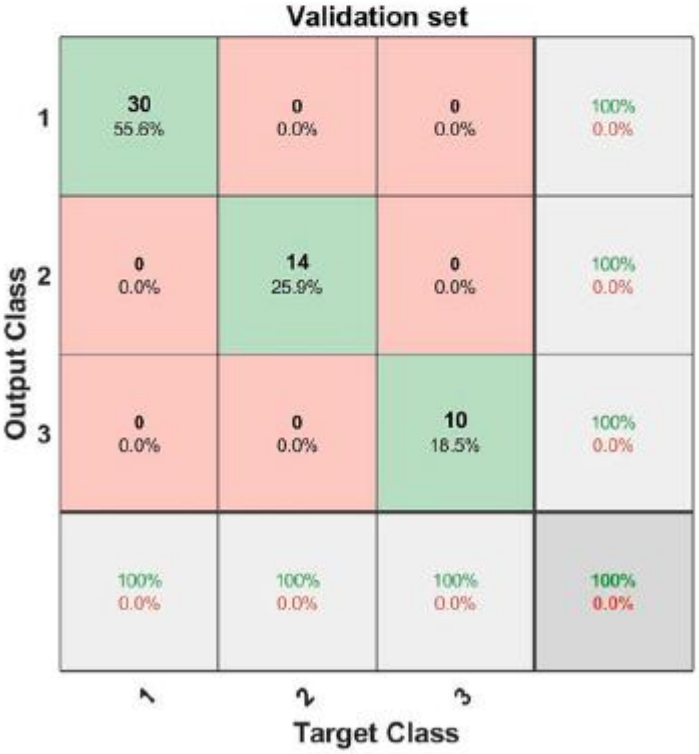
Validation set
30
55.6%
0
0.0%
0
0.0%
100%
0.0%
0
0.0%
14
25.9%
0
0.0%
100%
0.0%
0
0.0%
0
0.0%
10
18.5%
100%
0.0%
100%
0.0%
100%
0.0%
100%
0.0%
100%
0.0%
100%
0.0%
Output Class
1
2
3
Target Class
1
2
3

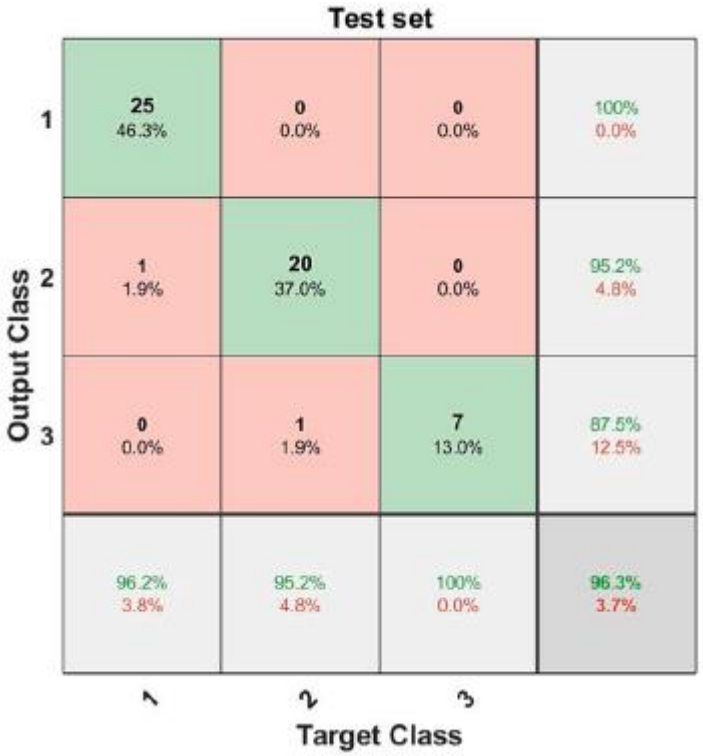

Figure 14 *The obtained training, validation, and test matrixes for classification based on floatability (120)*

The training, validation, and test matrices datasets enable the development and evaluation of machine learning models that aim to distinguish between different floating behaviors, supporting predictive formulation design.

The classification based on the input dataset created from the measured heights of the samples was performed using K-nearest neighbor classifier. The measured height values are illustrated in Figure 15. Based on this, four groups can be observed, comprising the 10 N (T/I), 30-45 N (T/II), 75-100 N (T/III), and 170 N (T/V) samples. By applying height as a variable, it becomes possible to develop a model capable of classifying samples according to their floating properties. The matrixes obtained based on the measured heights used as input data are shown in Figure 16. Of the test set samples, 100% were assigned to the correct class, while the training set achieved a value of 98.4%.

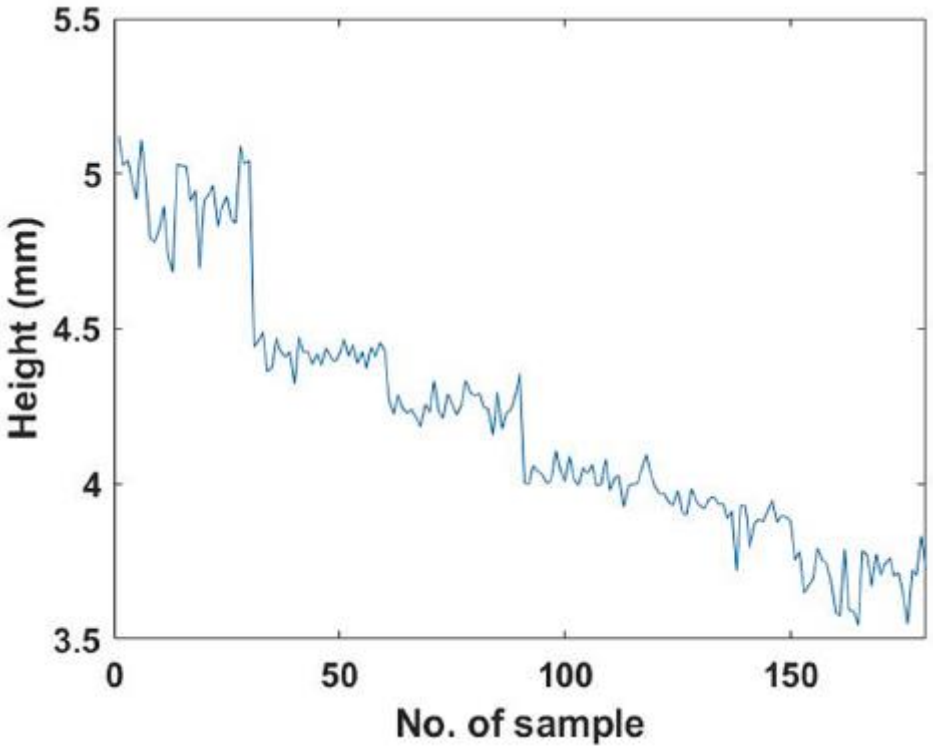

Figure 15 *The measured height of the samples (120)*

The image shows the measured height of the tablet samples with artificial neural networks, providing insight into their physical dimensions and potential correlations with compression force and floatability.

Figure 16 *The obtained confusion matrixes based on floatability (120)*

The images show the obtained confusion matrices for training and test sets in the classification task based on tablet floatability. These matrices visualize the model's ability to correctly identify floatable and non-floatable tablets, providing insight into classification accuracy and potential misclassifications across different data subsets.

Prediction accuracy of floating properties was approximately 100%, comparing the results of models based on measured height and imaging-based models. Ultimately, both approaches can be used to predict the special value.

4.2 Applicability of ICP-OES in in vitro drug release studies

As a model formulation, I used ibuprofen sodium-containing pellets. Since the pellets did not have any film coating, the solubility of the active ingredient in the medium determined the drug release profile. The results show that both measurement methods provided similar outcomes for immediate-release pellets (Figures 17 and 18). It is clearly visible that with both methods, more than 85% dissolution was observed after just one minute.

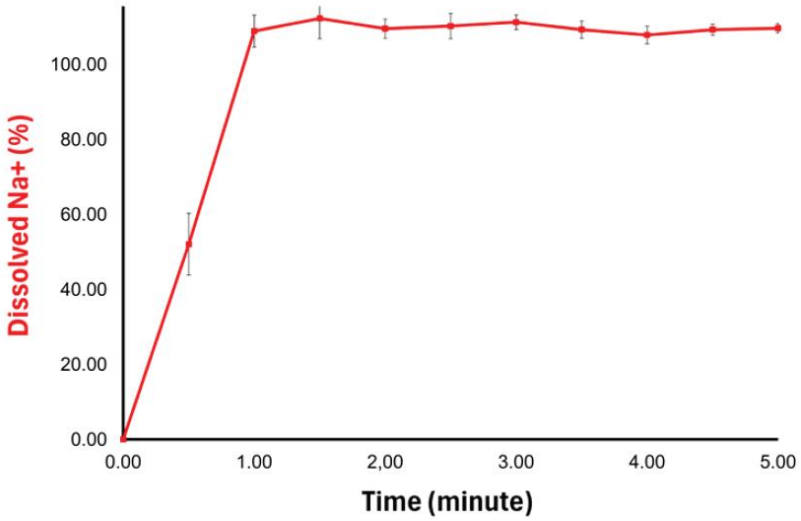

Figure 17 *Measurement of Na^+ dissolution with an ICP-OES device (own figure, 72)*

ICP-OES can detect trace elements with high precision and this image shows the release of sodium salt from ibuprofen sodium, which was monitored using an ICP-OES device.

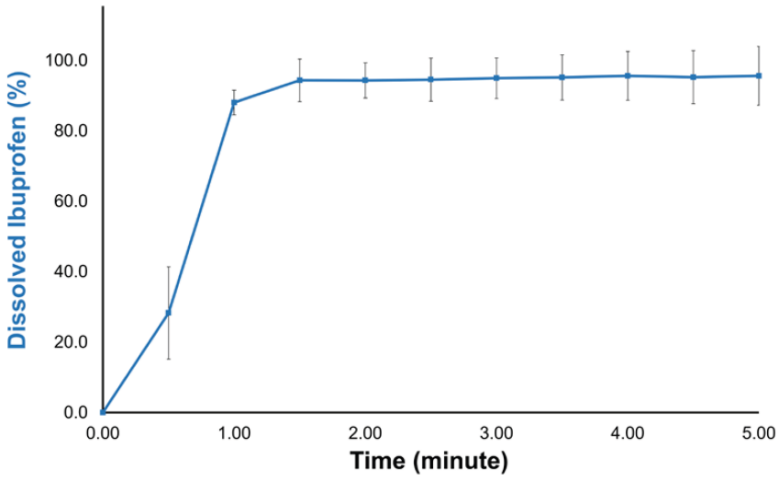

Figure 18 *Measurement of ibuprofen dissolution using fiber optic UV spectroscopy (own figure, 72)*

The ibuprofen-sodium is an immediate release (IR) tablet which dissolves rapidly, as reflected in this figure with Apparatus II.

To simulate oral drug administration, I applied for an innovative dosage form. To ensure that the experimental conditions closely resemble the processes occurring in the human body, I used a peristaltic pump to mimic the continuous flow rate found in the stomach, as well as the temporal changes in pH conditions. For the examination, the pellets were loaded into medicated straws through which the appropriate medium was circulated. Based on the results, it can be concluded that both ICP-OES in situ sample probing (Figure 19) and the In-Situ Fiber Optic UV System (Figure 20) are equally effective methods for determining salt concentration and active ingredient content from innovative dosage forms, such as medicated straws.

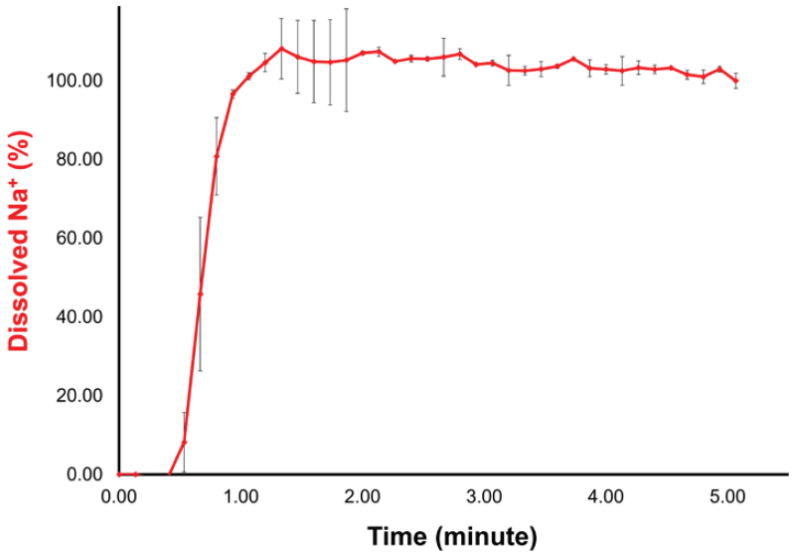

Figure 19 *Measurement of Na^+ concentration in medicated straws using an ICP-OES device (own figure, 72)*

The image demonstrates the applicability of ICP-OES for determining Na^+ concentration during an innovative drug administration method using a medicated straw.

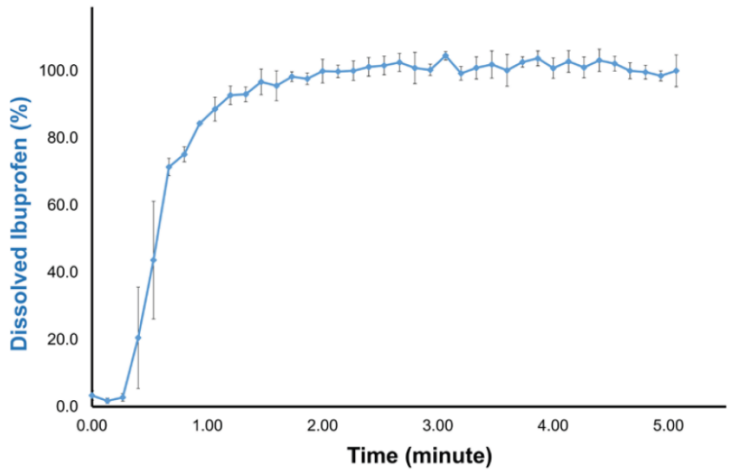

Figure 20 *Measurement of ibuprofen content in pellets loaded into straws using fiber optic UV spectroscopy (own figure, 72)*

The ibuprofen-sodium is an immediate release (IR) tablet which dissolves rapidly, as reflected in this figure using medicated straws.

5 Discussion

5.1 In vitro dissolution and floatability of floating tablets

5.1.1 Physical properties and content uniformity of tablets

To determine whether the compression force used during tableting affects crushing strength and floatability, I first prepared floating tablets using six different compression forces. To ensure a homogeneous powder blend for direct compression, I used Kollidon® SR and galenIQ™ 721 as excipients. My results also confirm the appropriate choice of excipients, as the tablets produced had suitable individual masses. As expected, increasing the compression force during tablet production increased the mechanical resistance as well as the density values. This is due to the fact that applying greater compression decreases the distance between solid particles, sometimes even causing fragmentation, so the particles are more densely placed in the tablet, increasing mechanical strength. As a result, the tablet compresses, its volume decreases, and its density increases. Furthermore, greater compression force reduces the porosity of the tablet, which also affects the dissolution profile. Content uniformity was not influenced by the varying compression force, as results always met requirements. This further confirms that my tablets were homogeneous.

5.1.2 In vitro drug release and determination of floatability by machine vision

To investigate the drug release profile and floating properties of the floating tablets, I used the Kollidon®

SR excipient system for tablet preparation, which possesses properties that influence floatability. It should be noted that physical parameters of the measured drug delivery system, such as tablet density and weight discussed in the previous section, may change upon contact with water. Kollidon® SR-based matrix tablets swell when in contact with water. The water-soluble components of the tablet (isomalt, povidone, API) dissolve, creating new pores in the water-insoluble poly(vinyl acetate) matrix. I determined drug release using in vitro dissolution testing and observed the tablets' floatability. Dissolution studies clearly showed that drug release was slower from tablets made with higher compression force. This is because increased compression reduces tablet porosity and, thus, decreases the rate of drug release.

During dissolution, tablets made with different compression forces floated and swelled differently in the dissolution medium. The tablet with the lowest calculated density (0.87 g/cm^3) floated on the surface from the beginning, while the one with the highest density (1.16 g/cm^3) remained at the bottom throughout. The others, being close to 1.0 g/cm^3, showed continuous movement within the medium. I precisely determined the tablets' position using image analysis.

Microscopic images were taken of the surfaces of tablets with different crushing strengths to enable their classification using artificial neural networks based on surface characteristics. The minor differences were caused by the API and specific excipients, which did not interfere with classification. Furthermore, this machine vision-based approach is suitable for predicting floatability, representing a fast, non-destructive method that can be used as a quality control step during manufacturing. Based on these findings, tablets with inadequate floatability can likely to be detected during production.

5.1.3 Classification based on crushing strength and floatability

Images were taken at specific time points during dissolution test, and these were used in imaging algorithms to assess the crushing strength and floatability of tablets made with different compression forces. Target classes had to be defined for classification, first according to crushing strength, for which there were six classes. Followed by three classes for floatability. According to the obtained confusion matrices, the misclassification rate was about 6% for crushing strength and only about 3% for floatability in the entire test set. These results demonstrate that the samples were successfully classified based on crushing strength and floatability using machine vision under visible illumination and pattern recognition neural networks.

When height was introduced as a new input, a model was created that could classify samples by floating properties. This method achieved approximately 100% prediction accuracy. Thus, either method can be used to predict the particular value.

5.2 Applicability of ICP-OES in in vitro drug release studies

In these experiments, I used immediate-release ibuprofen sodium pellet cores. Ibuprofen sodium (IBUNa) is a more soluble form than conventional ibuprofen, leading

to faster absorption and thus more rapid analgesic. To allow faster analgesic, new IBU preparations are designed to dissolve more easily in the stomach's acidic environment.

As it contains sodium salt, it was an ideal model compound to simultaneously determine both the active ingredient and its sodium salt using a dissolution apparatus and a highly sensitive ICP-OES instrument. My experiments achieved nearly identical results with both devices, indicating that ICP-OES and the fiber optic spectrophotometer are both effective in in vitro dissolution studies.

Additionally, to simulate drug administration, I used medicated straws. To better represent human physiology, I simulated continuous fluid flow rate and pH changes with a peristaltic pump. Pellets were loaded into the straws, and the appropriate medium was circulated through them. Based on my results, the method proved successful: both salt concentration and active ingredient content can be measured even through this innovative dosage form.

6 Conclusions

In the first part of my work, I analyzed the effect of various dissolution media on drug release. Subsequently, I focused on the significance and investigation of gastroretentive floating dosage forms. I used caffeine-containing floating tablets for in vitro dissolution studies, during which I examined their floatability and its temporal evolution to establish a relationship between drug release and floating properties. To this end, I first prepared tablets with equal composition but six different compression forces using direct compression, from which I concluded the floatability and dissolution rate based on hardness. Dissolution profiles support the theory that drug release is slower at higher compression forces. I thoroughly examined the tablets' physical parameters and calculated their density from available data (shape, height, weight), which supported the floatability and the slopes of the dissolution profiles. Microscopic images were taken of tablets with various crushing strengths, finding a correlation between surface gloss and hardness. During dissolution, I paid special attention not only to conventional pharmacopoeial tablet tests, but also to employing advanced image analysis techniques to observe the floating behavior of dosage forms, enabling precise tracking and prediction of floatability. For this, microscopic images of the tablets' surfaces and heights (thickness) were analyzed, beyond traditional tests (weight uniformity, crushing strength, disintegration, density), to uncover their floatability. The machine vision-based analysis demonstrated its suitability for predicting floatability, providing a rapid, non-destructive method applicable as a quality control step during manufacturing. Tablets with inadequate floating properties can thus be efficiently identified. For image data analysis, advanced image processing algorithms and artificial neural networks were used to classify and organize tablets by hardness and floatability. For classification, six classes were established based on measured crushing strengths, and three classes for floating evaluation. Successful application of the VIS imaging method was achieved, combined with pattern recognition neural networks, enabling precise classification of floating tablets according to their floatability. Additionally, the prediction accuracy of floating behavior was about 100% when a new model including height as an input was created. The results show that this combined approach offers a highly effective and rapid method

for examining tablet surfaces, enabling not only fast and non-destructive digital imaging, but also providing insights into mechanical and physical properties such as crushing strength and floating characteristics. In conclusion, this approach could enable faster and more reliable assessment of pharmaceutical formulation quality in the future, without causing any adverse effects in the samples. Its widespread application may contribute to the advancement of the pharmaceutical industry and the optimization of dosage forms.

The next phase of my work focused on studying the applicability of ICP-OES in conjunction with in vitro drug release studies, as this method holds remarkable potential for ensuring the safety and efficacy of pharmaceutical preparations. Qualitative and quantitative determination is critical for proper drug manufacturing and application, and the high sensitivity of ICP-OES enables precise measurement results. For the experiments, I prepared immediate-release ibuprofen sodium pellet cores, determining drug release and sodium concentration. The experiments and results indicate that ICP-OES and fiber optic UV spectroscopy provided similar results in in vitro dissolution, supporting the reliability and applicability of both methods. The similarity in outcomes confirms that ICP-OES successfully determines salt concentration and offers a well-applicable technique alongside traditional dissolution testing methods.

In further experiments, ibuprofen sodium pellet cores were loaded into straws to simulate an innovative drug administration possibility. A peristaltic pump was used to simulate continuous flow rate and pH changes, creating more biorelevant conditions that better model the environment of the human digestive system. This approach represents an important advance in simulating human conditions and may help better understand the release mechanisms of dosage forms. Using this experimental method, it was demonstrated that both ICP-OES in line sampling and in situ fiber optic UV spectroscopy are effective for testing even innovative dosage forms. The results confirm that these methods are not only highly precise but also applicable under more biorelevant conditions, thus contributing to the development and deeper understanding of pharmaceutical preparations. The research suggests that these techniques offer significant potential for pharmaceutical development and could further contribute to quality control and development processes in the pharmaceutical industry.

7 Summary

During my research, one of my main objectives was to explore the application of a rapid and non-destructive method capable of predicting the buoyancy properties of tablets. To achieve this, I first examined the effect of various dissolution media on drug release. Subsequently, I investigated gastroretentive floating drug delivery systems using in vitro dissolution studies to monitor their floating behavior and its progression over time. For this purpose, I prepared directly compressed caffeine-containing tablets with identical composition but using different compression forces. Based on the hardness of these tablets, I inferred their floating characteristics and drug release rates.

I calculated the density of the tablets using their physical parameters - shape, height, and weight - to support their influence on buoyancy. Microscopic images of the tablet surfaces were also taken, and I correlated surface gloss with tablet hardness. My research demonstrated that, in addition to determining physical parameters, microscopic imaging can be used to predict the buoyancy of floating tablets. Consequently, the dissolution profile may also be predicted. The procedure is fast, non-destructive, and may be suitable for quality control of floating tablets, through which tablets with altered floating properties resulting from manufacturing deviations can likely be detected. Furthermore, image processing algorithms and artificial neural networks were employed to classify the tablets based on their hardness and buoyancy.

The next phase of my work focused on evaluating the applicability of ICP-OES in combination with in vitro drug release testing. In this experiment, I prepared immediate-release ibuprofen sodium pellet cores as a model compound and simultaneously determined drug release and sodium concentration in-line. The results confirmed that both methods yielded comparable outcomes. Additionally, I successfully simulated an innovative drug delivery approach using pellets loaded into a straw. To mimic continuous flow and dynamic pH changes, a peristaltic pump was used, creating more biorelevant conditions.

8 References

1. Pillay V, Fassihi R. Evaluation and comparison of dissolution data derived from different modified release dosage forms: an alternative method. Journal of Controlled Release. 1998 Oct;55(1):45–55.
2. Al-Gousous J, Tsume Y, Fu M, Salem II, Langguth P. Unpredictable Performance of pH-Dependent Coatings Accentuates the Need for Improved Predictive *in Vitro* Test Systems. Mol Pharmaceutics. 2017 Dec 4;14(12):4209–19.
3. Lennernäs H, Abrahamsson B, Persson EM, Knutson L. Oral drug absorption and the Biopharmaceutics Classification System. Journal of Drug Delivery Science and Technology. 2007;17(4):237–44.
4. Dressmann JB, Amidon GL, Reppas C, Shah VP. Dissolution Testing as a Prognotic Tool for Oral Drug Absorption: Immediate Release Dosage Forms. Pharmaceutical Research, 1998.
6. Committee for Medicinal Products for Human use, EMA Guideline on the investigation of bioequivalence.
7. FDA. Bioequivalence studies with pharmacokinetic endpoints for drugs submitted under an ANDA. 2013.
8. Mandal UK, Chatterjee B, Senjoti FG. Gastro-retentive drug delivery systems and their in vivo success: A recent update. Asian Journal of Pharmaceutical Sciences. 2016 Oct;11(5):575–84.
9. Gröning R, Heun G. Oral Dosage Forms with Controlled Gastrointestinal Transit. Drug Development and Industrial Pharmacy. 1984 Jan;10(4):527–39.
10. Deshpande AA, Rhodes CT, Shah NH, Malick AW. Controlled-Release Drug Delivery Systems for Prolonged Gastric Residence: An Overview. Drug Development and Industrial Pharmacy. 1996 Jan;22(6):531–9.
11. Altreuter DH, Kirtane AR, Grant T, Kruger C, Traverso G, Bellinger AM. Changing the pill: developments toward the promise of an ultra-long-acting gastroretentive dosage form. Expert Opinion on Drug Delivery. 2018 Dec 2;15(12):1189–98.
12. Chavanpatil MD, Jain P, Chaudhari S, Shear R, Vavia PR. Novel sustained release, swellable and bioadhesive gastroretentive drug delivery system for ofloxacin. International Journal of Pharmaceutics. 2006 Jun;316(1–2):86–92.

13. Amidon GL, Lennernäs H, Shah VP and Crison JR. A Theoretical Basis for a Biopharmaceutic Drug Classification: The Correlation of in Vitro Drug Product Dissolution and in Vivo Bioavailability. Pharmaceutical Research., pp. 12 (3), 413-420., 1995.
14. Kakuk M, Farkas D, Antal I, Kállai-Szabó N. Advances in drug release investigations: Trends and developments for dissolution test media. APH. 2020 Dec 24;90(4):155–69.
15. Reddy BBK, Karunakar A. Biopharmaceutics Classification System: A Regulatory Approach. Dissolution Technol. 2011;18(1):31–7.
16. Kasim NA, Whitehouse M, Ramachandran C, Bermejo M, Lennernäs H, Hussain AS, et al. Molecular Properties of WHO Essential Drugs and Provisional Biopharmaceutical Classification. Mol Pharmaceutics. 2004 Jan 1;1(1):85–96.
17. Morais JAG, Lobato MDR. The New European Medicines Agency Guideline on the Investigation of Bioequivalence. Basic Clin Pharma Tox. 2010 Mar;106(3):221–5.
18. Avdeef A. Absorption and Drug Development: Solubility, Permeability, and Charge State [Internet]. 1st ed. Wiley; 2003 [cited 2024 Dec 2]. Available from: https://onlinelibrary.wiley.com/doi/book/10.1002/047145026X
19. Lipinski CA, Lombardo F, Dominy BW, Feeney PJ. Experimental and Computational Approaches to Estimate Solubility and Permeability in Drug Discovery and Development Settings. Advanced Drug Delivery Reviews., pp. 64, 4-17., 2012.. https://doi.org/10.1016/j.addr.2012.09.019
20. Serajuddin ATM. Salt Formation to Improve Drug Solubility. ChemInform. 2007 Dec 25;38(52):chin.200752235.
21. Yu LX, Amidon GL, Polli JE, Zhao H, Mehta MU, Conner DP, et al. Biopharmaceutics Classification System: The Scientific Basis for Biowaiver Extensions.
22. Dahan A, Miller JM, Amidon GL. Prediction of Solubility and Permeability Class Membership: Provisional BCS Classification of the World's Top Oral Drugs. AAPS J. 2009 Dec;11(4):740–6.

23. Thayer AM. Finding Solutions: Custom manufacturers take on drug solubilitiy issues to help pharmaceutical firms move products through development. Chem Eng News Archive. 2010 May 31;88(22):13–8.
24. Polli JE, Abrahamsson BSI, Yu LX, Amidon GL, Baldoni JM, Cook JA, et al. Summary Workshop Report: Bioequivalence, Biopharmaceutics Classification System, and Beyond. AAPS J. 2008 Jun;10(2):373–9.
25. Butler JM, Dressman JB. The Developability Classification System: Application of Biopharmaceutics Concepts to Formulation Development. Journal of Pharmaceutical Sciences, 2010 Dec;99:12.
26. Rosenberger J, Butler J, Dressman J. A Refined Developability Classification System. Journal of Pharmaceutical Sciences . 2018 Aug;2020-2032.
27. Jorgensen ED, Bhagwat D. Development of dissolution tests for oral extended-release products. Pharmaceutical Science & Technology Today. 1998 Jun;1(3):128–35.
28. Noyes AA, Whitney WR. The rate of solution of solid substances in their own solutions. J Am Chem Soc. 1897 Dec;19(12):930–4.
29. Danckwerts PV. Significance of Liquid-Film Coefficients in Gas Absorption. Ind Eng Chem. 1951 Jun;43(6):1460–7.
30. Dokoumetzidis A, Macheras P. A century of dissolution research: From Noyes and Whitney to the Biopharmaceutics Classification System. International Journal of Pharmaceutics. 2006 Sep;321(1–2):1–11.
31. Gershberg S, Stoll FD. Apparatus, for Tablet Disintegration, and for Shaking-Out Extractions.*. Journal of the American Pharmaceutical Association (Scientific ed). 1946 Sep;35(9):284–7.
32. Chapman DG, Crisafio R, Campbell JA. The Relation Between in Vitro Disintegration Time of Sugar-Coated Tablets and Physiological Availability of Riboflavin*. Journal of the American Pharmaceutical Association (Scientific ed). 1954 May;43(5):297–304.
33. Filleborn VM. A new approach to tablet disintegration testing. American journal of pharmacy and the sciences supporting public health. 1948;120(7):233-55.
34. Dressman J, Krämer J. Pharmaceutical Dissolution Testing. 2005;

35. Edwards LJ. The dissolution and diffusion of aspirin in aqueous media. Trans Faraday Soc. 1951;47:1191.
36. Nelson E. Solution Rate of Theophylline Salts and Effects from Oral Administration**School of Pharmacy, University of California Medical Center, San Francisco 22. Journal of the American Pharmaceutical Association (Scientific ed). 1957 Oct;46(10):607–14.
37. Campagna FA, Cureton G, Mirigian RA, Nelson E. Inactive Prednisone Tablets U.S.P. XVI. Journal of Pharmaceutical Sciences. 1963 Jun;52(6):605–6.
38. Levy G, Hall NA, Nelson E. Studies on Inactive Prednisone Tablets, U.S.P. XVI. American Journal of Health-System Pharmacy. 1964 Sep 1;21(9):402–402.
39. Levy G. Effect of Dosage Form Properties on Therapeutic Efficacy of Tolbutamide Tablets. Can Med Assoc J. 1964 Apr 18;90(16):978–9.
40. Mudie DM, Murray K, Hoad CL, Pritchard SE, Garnett MC, Amidon GL, et al. Quantification of Gastrointestinal Liquid Volumes and Distribution Following a 240 mL Dose of Water in the Fasted State. Mol Pharmaceutics. 2014 Sep 2;11(9):3039–47.
41. Martin CM, Rubin M, O'Malley WG, V. F. Garagusi, C. E. McCauley, "Brand, generic drugs differ in man," Journal of the Americal Association , p. 205, 1968.
42. Fraser EJ, Leach RH, Poston JW. Bioavailability of digoxin. Lancet 2, p. 541, 1972. https://doi.org/10.1016/S0140-6736(72)91936-8
43. Tyrer JH, Eadie MJ, Sutherland JM, Hooper WD. Outbreak of Anticonvulsant Intoxication in an Australian City. Br Med J. 1970 Oct 31;4(5730):271–3.
44. Bochner F, Hooper WD, Tyrer JH, Eadie MJ. Factors involved in an outbreak of phenytoin intoxication. Journal of the Neurological Sciences. 1972 Aug;16(4):481–7.
45. Garnett WR, Carter BL, Pellock JM. Effect of Calcium and Antacids on Phenytoin Bioavailability. Archives of Neurology. 1980 Jul 1;37(7):467–467.
46. Marroum PJ. History and Evolution of the Dissolution Test. Dissolution Technol. 2014;21(3):11–6.

47. Európai Gyógyszerkönyv. Szilárd gyógyszerformák kioldódási vizsgálata (2.9.3). Európai Gyógyszerkönyv 11. Kiadás, Európai Gyógyszerkönyv Bizottság. Strasbourg, Franciaország, 2023; 348.
48. Soltero RA, Hoover JM, Jones TF, Standish M. Effects of Sinker Shapes on Dissolution Profiles. Journal of Pharmaceutical Sciences. 1989 Jan;78(1):35–9.
49. Bredael G, Liang S, Hahn D. A Strategy for Quality Control Dissolution Method Development for Immediate-Release Solid Oral Dosage Forms. Dissolution Technol. 2015;22(3):10–6.
50. Beckett AH, Quach TT, Kurs GS. Improved Hydrodynamics for USP Apparatus 2. Dissolution Technol. 1996;3(2):7–18.
51. Borst I, Ugwu S, Beckett AH. New and Extended Applications for USP Drug Release Apparatus 3. Dissolution Technol. 1997;4(1):11–8.
52. Pezzini BR, Issa MG, Duque MD, Ferraz HG. Applications of USP apparatus 3 in assessing the in vitro release of solid oral dosage forms. Braz J Pharm Sci. 2015 Jun;51(2):265–72.
53. Gray V. Handbook of Dissolution Testing. 2004.
54. Singh I, Aboul-Enein HY. Advantages of USP Apparatus IV (flow-through cell apparatus) in dissolution studies. JICS. 2006 Sep;3(3):220–2.
55. Deglaire A, Bos C, Tomé D, Moughan PJ. Ileal digestibility of dietary protein in the growing pig and adult human. Br J Nutr. 2009 Dec 28;102(12):1752–9.
56. Hanks JH, Wallace RE. Relation of Oxygen and Temperature in the Preservation of Tissues by Refrigeration. Proceedings of the Society for Experimental Biology and Medicine. 1949 Jun 1;71(2):196–200.
57. Liu F, Merchant HA, Kulkarni RP, Alkademi M, Basit AW. Evolution of physiological pH 6.8 bicarbonate buffer systems: application to the.
58. Merchant HA, Goyanes A, Parashar N, Basit AW. Predicting the gastrointestinal behaviour of modified-release products: Utility of a novel dynamic dissolution test apparatus involving the use of bicarbonate buffers. International Journal of Pharmaceutics. 2014 Nov;475(1–2):585–91.

59. Fadda HM, Merchant HA, Arafat BT, Basit AW. Physiological bicarbonate buffers: stabilisation and use as dissolution media for modified release systems. International Journal of Pharmaceutics. 2009 Dec;382(1–2):56–60.
60. Garbacz G, Kolodziej B, Koziolek M, Weitschies W, Klein S. A dynamic system for the simulation of fasting luminal pH-gradients using hydrogen carbonate buffers for dissolution testing of ionisable compounds. European Journal of Pharmaceutical Sciences, pp. 51, 224−231, 2014. https://doi.org/10.1016/j.ejps.2013.09.020
61. Garbacz G, Kołodziej B, Koziolek M, Weitschies W, Klein S. An Automated System for Monitoring and Regulating the pH of Bicarbonate Buffers. AAPS PharmSciTech. 2013 Mar 7;14(2):517–22.
62. Al-Gousous J, Amidon GL, Langguth P. Toward Biopredictive Dissolution for Enteric Coated Dosage Forms. Mol Pharmaceutics. 2016 Jun 6;13(6):1927–36.
63. Al-Gousous J, Amidon GL, Langguth P. Toward Biopredictive Dissolution for Enteric Coated Dosage Forms. Mol Pharmaceutics. 2016 Jun 6;13(6):1927–36.
64. Shohin IE, Grebenkin DYu, Malashenko EA, Stanishevskii YaM, Ramenskaya GV. A Brief Review of the FDA Dissolution Methods Database. Dissolution Technol. 2016;23(3):6–10.
65. Steingoetter A, Fox M, Treier R, Weishaupt D, Marincek B, Boesiger P, et al. Effects of posture on the physiology of gastric emptying: A magnetic resonance imaging study. Scandinavian Journal of Gastroenterology. 2006 Jan;41(10):1155–64.
66. Argon M, Duygun U, Daglioz G, Om??r O, Demir E, Aydogdu S. Relationship Between Gastric Emptying and Gastroesophageal Reflux in Infants and Children: Clinical Nuclear Medicine. 2006 May;31(5):262–5.
67. Galia E, Horton J, Dressman JB. Albendazole Generics—A Comparative In Vitro Study. Pharm Res. 1999 Dec 1;16(12):1871–5.
68. Fallingborg J, Christensen LA, Ingeman-Nielsen M, Jacobsen BA, Abildgaard K, Rasmussen HH, et al. Measurement of Gastrointestinal pH and Regional Transit Times in Normal Children: Journal of Pediatric Gastroenterology and Nutrition. 1990 Aug;11(2):211–4.

69. Fallingborg J, Christensen LA, Ingeman-Nielsen M, Jacobsen BA, Abildgaard K, Rasmussen HH. pH-Profile and regional transit times of the normal gut measured by a radiotelemetry device. Aliment Pharmacol Ther. 1989 Dec;3(6):605–14.
70. McConnell EL, Fadda HM, Basit AW. Gut instincts: Explorations in intestinal physiology and drug delivery. International Journal of Pharmaceutics. 2008 Dec;364(2):213–26.
71. Maharaj AR, Edginton AN, Fotaki N. Assessment of Age-Related Changes in Pediatric Gastrointestinal Solubility. Pharm Res. 2016 Jan;33(1):52–71.
72. Kakuk M, Farkas D, Kállai-Szabó B, Pencz K, Mészáros LA, Tonka-Nagy PG, Kállai-Szabó N, Antal I, Inductively Coupled Plasma Optical Emission Spectroscopy (ICP-OES): Exploring Versatile Applications in Industrial and Analytical Fields. Periodica Polytech. Chem. Engin. 2025. Jun 12.
73. Singla N, Gupta GD, Kohli K, Singla AK. A Discriminatory and Biorelevant Dissolution Test Method for Simvastatin Drug Products. Dissolution Technol. 2009;16(4):11–3.
74. Klein S. The Use of Biorelevant Dissolution Media to Forecast the In Vivo Performance of a Drug. AAPS J. 2010 Sep;12(3):397–406.
75. Evaluation-of-Various-Dissolution-Media_1998.pdf [Internet]. [cited 2024 Dec 3]. Available from: https://biorelevant.com/site_media/upload/literature/Evaluation-of-Various-Dissolution-Media_1998.pdf
76. Sheng JJ, McNamara DP, Amidon GL. Toward an *In Vivo* Dissolution Methodology: A Comparison of Phosphate and Bicarbonate Buffers. Mol Pharmaceutics. 2009 Feb 2;6(1):29–39.
77. Otsuka K, Shono Y, Dressman J. Coupling biorelevant dissolution methods with physiologically based pharmacokinetic modelling to forecast in-vivo performance of solid oral dosage forms. Journal of Pharmacy and Pharmacology. 2013 Jun 6;65(7):937–52.
78. Carino SR, Sperry DC, Hawley M. Relative bioavailability estimation of carbamazepine crystal forms using an artificial stomach-duodenum model. Journal of Pharmaceutical Sciences. 2006 Jan;95(1):116–25.

79. Mudie DM, Amidon GL, Amidon GE. Physiological Parameters for Oral Delivery and *in Vitro* Testing. Mol Pharmaceutics. 2010 Oct 4;7(5):1388–405.
80. Takeuchi S, Tsume Y, Amidon GE, Amidon GL. Evaluation of a Three Compartment In Vitro Gastrointestinal Simulator Dissolution Apparatus to Predict In Vivo Dissolution. Journal of Pharmaceutical Sciences. 2014 Nov;103(11):3416–22.
81. Mwilu SK, El Badawy AM, Bradham K, Nelson C, Thomas D, Scheckel KG, et al. Changes in silver nanoparticles exposed to human synthetic stomach fluid: Effects of particle size and surface chemistry. Science of The Total Environment. 2013 Mar;447:90–8.
82. Rogers KR, Bradham K, Tolaymat T, Thomas DJ, Hartmann T, Ma L, et al. Alterations in physical state of silver nanoparticles exposed to synthetic human stomach fluid. Science of The Total Environment. 2012 Mar;420:334–9.
83. Kalantzi L, Goumas K, Kalioras V, Abrahamsson B, Dressman JB, Reppas C. Characterization of the Human Upper Gastrointestinal Contents Under Conditions Simulating Bioavailability/Bioequivalence Studies. Pharm Res. 2006 Jan;23(1):165–76.
84. Jantratid E, De Maio V, Ronda E, Mattavelli V, Vertzoni M, Dressman JB. Application of biorelevant dissolution tests to the prediction of in vivo performance of diclofenac sodium from an oral modified-release pellet dosage form. European Journal of Pharmaceutical Sciences. 2009 Jun;37(3–4):434–41.
85. Hollebeeck S, Borlon F, Schneider YJ, Larondelle Y, Rogez H. Development of a standardised human in vitro digestion protocol based on macronutrient digestion using response surface methodology. Food Chemistry. 2013 Jun;138(2–3):1936–44.
86. Versantvoort CHM, Oomen AG, Van De Kamp E, Rompelberg CJM, Sips AJAM. Applicability of an in vitro digestion model in assessing the bioaccessibility of mycotoxins from food. Food and Chemical Toxicology. 2005 Jan;43(1):31–40.
87. Vertzoni M, Dressman J, Butler J, Hempenstall J, Reppas C. Simulation of fasting gastric conditions and its importance for the in vivo dissolution of lipophilic compounds. European Journal of Pharmaceutics and Biopharmaceutics. 2005 Aug;60(3):413–7.

88. Macheras P, Koupparis M, Tsaprounis C. Drug dissolution studies in milk using the automated flow injection serial dynamic dialysis technique. International Journal of Pharmaceutics. 1986 Nov;33(1–3):125–36.
89. Macheras P, Koupparis M, Apostolelli E. Dissolution of 4 controlled-release theophylline formulations in milk. International Journal of Pharmaceutics. 1987 Apr;36(1):73–9.
90. Macheras PE, Koupparis MA, Antimisiaris SG. Effect of Temperature and Fat Content on the Binding of Hydrochlorothiazide and Chlorothiazide to Milk. Journal of Pharmaceutical Sciences. 1988 Apr;77(4):334–6.
91. Macheras P, Koupparis M, Antimisiaris S. An in vitro model for exploring CR theophylline-milk fat interactions. International Journal of Pharmaceutics. 1989 Sep;54(2):123–30.
92. Jantratid E, Janssen N, Reppas C, Dressman JB. Dissolution Media Simulating Conditions in the Proximal Human Gastrointestinal Tract: An Update. Pharm Res. 2008 Jul;25(7):1663–76.
93. Dressman JB, Vertzoni M, Goumas K, Reppas C. Estimating drug solubility in the gastrointestinal tract. Advanced Drug Delivery Reviews. 2007 Jul;59(7):591–602.
94. Dressman JB, Berardi RR, Dermentzoglou LC, Russell TL, Schmaltz SP, Barnett JL, Jarvenpaa KM. Upper Gastrointestinal (GI) pH in Young, Healthy Men and Women. Phamaceutical Research, 1990.
95. Passannanti F, Nigro F, Gallo M, Tornatore F, Frasso A, Saccone G, et al. In vitro dynamic model simulating the digestive tract of 6-month-old infants. Passi AG, editor. PLoS ONE. 2017 Dec 20;12(12):e0189807.
96. Van Der Vossen AC, Hanff LM, Vulto AG, Fotaki N. Potential prediction of formulation performance in paediatric patients using biopharmaceutical tools and simulation of clinically relevant administration scenarios of nifedipine and lorazepam. Brit J Clinical Pharma. 2019 Aug;85(8):1728–39.
97. Nicolaides E, Galia E, Efthymiopoulos C, Dressman JB, Reppas C. Forecasting the In Vivo Performance of Four Low Solubility Drugs from Their In Vitro Dissolution Data. Pharmaceutical Research, 1999.

98. Evans DF, Pye G, Bramley R, Clark AG, Dyson TJ, Hardcastle JD. Measurement of gastrointestinal pH profiles in normal ambulant human subjects. Gut. 1988 Aug 1;29(8):1035–41.
99. Koziolek M, Grimm M, Becker D, Iordanov V, Zou H, Shimizu J, et al. Investigation of pH and Temperature Profiles in the GI Tract of Fasted Human Subjects Using the Intellicap® System. Journal of Pharmaceutical Sciences. 2015 Sep;104(9):2855–63.
100. Kalantzi L, Persson E, Polentarutti B, Abrahamsson B, Goumas K, Dressman JB, Reppas C. Canine Intestinal Contents vs. Simulated Media for the Assessment of Solubility of Two Weak Bases in the Human Small Intestinal Contents. Research paper, 2006. https://doi.org/10.1007/s11095-006-0207-8
101. Vertzoni M, Fotaki N, Nicolaides E, Reppas C, Kostewicz E, Stippler E, et al. Dissolution media simulating the intralumenal composition of the small intestine: physiological issues and practical aspects. Journal of Pharmacy and Pharmacology. 2004 Apr 1;56(4):453–62.
102. Marques MC, Loebenberg R, Almukainzi M. Simulated Biological Fluids with Possible Application in Dissolution Testing. Dissolution Technologies, 2011. https://doi.org/10.14227/DT180311P15
103. Fotaki N, Symillides M, Reppas C. In vitro versus canine data for predicting input profiles of isosorbide-5-mononitrate from oral extended release products on a confidence interval basis. European Journal of Pharmaceutical Sciences. 2005 Jan;24(1):115–22.
104. Graff J, Brinch K, Madsen JL. Gastrointestinal mean transit times in young and middle-aged healthy subjects. Clinical Physiology. 2001 Mar;21(2):253–9.
105. Algorri M, Cauchon NS, Christian T, O'Connell C, Vaidya P. Patient-Centric Product Development: A Summary of Select Regulatory CMC and Device Considerations. Journal of Pharm. Sciences. 2023; 112:4:922-936.
106. Bhutani U, Basu T, Majumdar S. Oral Drug Delivery: Conventional to Long Acting New-Age Designs. European Journal of Pharmaceutics and Biopharmaceutics. 2021 May;162:23–42.

107. Lou J, Duan H, Qin Q, Teng Z, Gan F, Zhou X, et al. Advances in Oral Drug Delivery Systems: Challenges and Opportunities. Pharmaceutics. 2023 Feb;15(2):484.
108. Omidian H, Park K. Oral Targeted Drug Delivery Systems: Gastric Retention Devices. Oral Controlled Release Formulation Design and Drug Delivery: Theory to Practice. 2010. 185-203.
109. Wang S, Wen H, Li P, Cui M, Sun W, Wang H, et al. Formulation and evaluation of gastric-floating controlled release tablets of Ginkgolides. Journal of Drug Delivery Science and Technology. 2019 Jun;51:7–17.
110. Timmermans J, Moës AJ. How well do floating dosage forms float? International Journal of Pharmaceutics. 1990 Jul;62(2–3):207–16.
111. Omidian H, Park K. Oral Targeted Drug Delivery Systems: Gastric Retention Devices. In: Wen H, Park K, editors. Oral Controlled Release Formulation Design and Drug Delivery [Internet]. 1st ed. Wiley; 2010 [cited 2024 Dec 2]. p. 185–203. https://doi.org/10.1002/9780470640487.ch12.
112. Chen N, Niu J, Li Q, Li J, Chen X, Ren Y, et al. Development and evaluation of a new gastroretentive drug delivery system: Nanomicelles-loaded floating mucoadhesive beads. Journal of Drug Delivery Science and Technology. 2019 Jun;51:485–92.
113. Rahamathulla M, Alshahrani SM, Al Saqr A, Alshetaili A, Shakeel F. Effervescent floating matrix tablets of a novel anti-cancer drug neratinib for breast cancer treatment. Journal of Drug Delivery Science and Technology. 2021 Dec;66:102788.
114. Huanbutta K, Sriamornsak P, Kittanaphon T, Suwanpitak K, Klinkesorn N, Sangnim T. Development of a zero-order kinetics drug release floating tablet with anti–flip-up design fabricated by 3D-printing technique. J Pharm Investig. 2021 Mar;51(2):213–22.
115. Baumgartner S, Kristl J, Vreˇcer F, Vodopivec P, Zorko B. Optimisation of floating matrix tablets and evaluation of their gastric residence time, Int. J. Pharm. 195 (1–2) (2000) 125–135, https://doi.org/10.1016/S0378-5173(99)00378-6.

116. Galata DL, Mészáros LA, Kállai-Szabó N, Szabó E, Pataki H, Marosi G, et al. Applications of machine vision in pharmaceutical technology: A review. European Journal of Pharmaceutical Sciences. 2021 Apr;159:105717.
117. Wahlich J. Review: Continuous Manufacturing of Small Molecule Solid Oral Dosage Forms. Pharmaceutics. 2021 Aug 22;13(8):1311.
118. Rangarao K, Padmalathadevi K. Swelling controlled-release systems: recent developments and applications. International Journal of Pharmaceutics. 1988 Dec;48(1–3):1–13.
119. Mészáros LA, Galata DL, Madarász L, Köte Á, Csorba K, Dávid ÁZ, et al. Digital UV/VIS imaging: A rapid PAT tool for crushing strength, drug content and particle size distribution determination in tablets. International Journal of Pharmaceutics. 2020 Mar;578:119174.
120. Kakuk M, Mészáros LA, Farkas D, Tonka-Nagy P, Tóth B, Nagy ZsK, Antal I, Kállai-Szabó N. Evaluation of floatability characteristics of gastroretentive tablets using VIS imaging with artificial neural networks. European Journal of Pharmaceutics and Biopharmaceutics. 2024 Sept 6; 90:155-169. DOI: 10.1016/j.ejpb.2024.114493.
121. Thapa P, Jeong SH. Effects of Formulation and Process Variables on Gastroretentive Floating Tablets with A High-Dose Soluble Drug and Experimental Design Approach. Pharmaceutics. 2018 Sep 17;10(3):161.
122. Iglesias N., Galbis E., Azogil L.R., Benito E., Lucas R., Gracia M., Violante de Paz M. In-Depth Study into Polymeric Materials in Low-Density Gastroretentive Formulations. Pharmaceutics. 2020. 12(7),636. DOI: 10.3390/pharmaceutics12070636
123. Rahim S.A., Carter P.A., Elkordy A.A. Design and evaluation of effervescent floating tablets based on hydroxyethyl cellulose and sodium alginate using pentoxifylline as a model drug. Drug Design, Development an Therapy. 2015. 1843-1857. DOI: 10.2147/DDDT.S78717.
124. Kim B., Byun Y., Lee E.H. DoE-Based Design of a Siple but Efficient Preparation Method for a Non-Effervescent Gastro.Retentive Floating Tablet Containing

Metformin HCl. Pharmaceutics. 2021. 13(8),1225. DOI: 10.3390/pharmaceutics13081225

125. Gad S, Heikal E, Hamadi T. Bioadhesive Drug Delivery Systems: A Review. Records of Pharmaceutical and Biomedical Sciences. 2023 Jan 1;7(3):25–40.
126. Klausner EA, Eyal S, Lavy E, Friedman M, Hoffman A. Expandable gastroretentive dosage forms. J Con Rel, 2003. 88:117-126.
127. Keogh JP. Membarne Transporters in Drug Development. Advances in Pharmacology, 2012 (63). http://dx.doi.org/10.1016/B978-0-12-398339-8.00001-X.
128. Talukder R., Fassihi R. Gastroretentive Delivery Systems: A Mini Review. Drug Development and Industrial Pharmacy. 2004. 30(10):1019-1028.
129. Omidian H., Rocca J.G., Park K. Advances in superporous hydrogels. Journal of Controlled Release. 2004. 102, 3-12.
130. Brinck C., Mark E.B., Klinge M.W., Ejerskov C., Sutter N., Schlageter V., Scott S.M., Drewes A.M., Krogh K. Magnetic tracking of gastrointestinal motility. Physiological Measurement. 2020.
131. Guo X., Chang R.K., Hussain M.A. Ion-Exchange Resins as Drug Delivery Carriers. Journal of Pharmaceutical Sciences. 2009. 98(11).
132. Wesolowski M, Suchacz B. Artificial Neural Networks: Theoretical Background and Pharmaceutical Applications: A Review. Journal of AOAC International. 2012; 95:3.
133. Teja TB, Sekar M, Pallavin T, Mettu S, Murthy TEG, Rani NNIM, Bra,hachari PV, Bonam SR. Role of Artificial Neural Networks in Pharmaceutical Sciences. J Young Pharm., 2022; 14(1):6-14.
134. Farkas B., Balogh A., Farkas A., Domokos A., Borbás E., Marosi G., Nag, ZK. Medicated Straws Based on Electrospun Solid Dispersions. Periodica Polytechnica Chemical Engineering, 62(3), pp. 310–316, 2018. https://doi.org/10.3311/PPch.11931
135. Király M, Sántha K, Kállai-Szabó B, Pencz KM, Ludányi K, Kállai-Szabó N, et al. Development and Dissolution Study of a β-Galactosidase Containing Drinking Straw. Pharmaceutics. 2022 Mar 31;14(4):769.

136. European Pharmacopoeia Commission. UNIFORMITY OF DOSAGE UNITS (2.9.40). In European Pharmacopoeia, 11th ed.; European Pharmacopoeia Commission: Strasbourg, France, 2023; pp. 421.
137. European Pharmacopoeia Commission. FRIABILITY OF UNCOATED TABLETS (2.9.7). In European Pharmacopoeia, 11th ed.; European Pharmacopoeia Commission: Strasbourg, France, 2023; pp. 359.
138. Spectrophotometric Analysis of Ibuprofen According to USP and EP Monographs. ThermoFisher Scientific.
139. Obeidat WM, Lahlouh IK, Gharaibeh SF. Investigations on Compaction Behavior of Kollidon® SR-Based Multi-component Directly Compressed Tablets for Preparation of Controlled Release Diclofenac Sodium. AAPS PharmSciTech. 2023 Nov 10;24(8):225.
140. Shergill M, Patel M, Khan S, Bashir A, McConville C. Development and characterisation of sustained release solid dispersion oral tablets containing the poorly water soluble drug disulfiram. International Journal of Pharmaceutics. 2016 Jan;497(1–2):3–11.
141. European Pharmacopoeia Commission. UNIFORMITY OF MASS OF SINGLE-DOSE PREPARATIONS (2.9.5). In European Pharmacopoeia, 11th ed.; European Pharmacopoeia Commission: Strasbourg, France, 2023; pp. 4523.
142. Chen D, Xu XY, Li R, Zang GA, Zhang Y, Wang MR, et al. Preparation and In vitro Evaluation of FDM 3D-Printed Ellipsoid-Shaped Gastric Floating Tablets with Low Infill Percentages. AAPS PharmSciTech. 2020 Jan;21(1):6.
143. Crișan AG, Porfire A, Iurian S, Rus LM, Lucăcel Ciceo R, Turza A, et al. Development of a Bilayer Tablet by Fused Deposition Modeling as a Sustained-Release Drug Delivery System. Pharmaceuticals. 2023 Sep;16(9):1321.
144. Nguyen TT, Hwang KM, Kim SH, Park ES. Development of novel bilayer gastroretentive tablets based on hydrophobic polymers. International Journal of Pharmaceutics. 2020 Jan 25;574:118865.
145. Iglesias N, Galbis E, Romero-Azogil L, Benito E, Lucas R, García-Martín MG, et al. In-Depth Study into Polymeric Materials in Low-Density Gastroretentive Formulations. Pharmaceutics. 2020 Jul 7;12(7):636.

9 Bibliography of the candidate's publications

9.1 Publication relevant to the dissertation

Kakuk M, Farkas D, Antal I, Kállai-Szabó N. Advances in drug release investigations Trends and developments for dissolution test. Acta Pharmaceutica Hungarica. 2020 Jul 17; 90:155-169. DOI: 10.33892/aph.2020.90.155-169.

Kakuk M, Mészáros LA, Farkas D, Tonka-Nagy P, Tóth B, Nagy ZsK, Antal I, Kállai-Szabó N. Evaluation of floatability characteristics of gastroretentive tablets using VIS imaging with artificial neural networks. European Journal of Pharmaceutics and Biopharmaceutics. 2024 Sept 6; 90:155-169. DOI: 10.1016/j.ejpb.2024.114493.

Kakuk M, Farkas D, Kállai-Szabó B, Pencz K, Mészáros LA, Tonka-Nagy P, Kállai-Szabó N, Antal I. Inductively Coupled Plasma Optical Emission Spectroscopy (ICP-OES): Exploring Versatile Applications in Industrial and Analytical Fields. Periodica Polytechnica Chemical Engineering. 2025. Jun 12. DOI: https://doi.org/10.3311/PPch.40025.

9.2 Other, not related publications

Katona MT, **Kakuk M**, Szabó R, Tonka-Nagy P, Takács-Novák K, Borbás E. Towards a Better Understanding of the Post-Gastric Behavior of Enteric-Coated Formulations. Pharmaceutical Research. 2022 Jan 18; DOI: 10.1007/s11095-021-03163-0.

10 Acknowledgements

I would like to express my heartfelt gratitude to Prof. Dr. István Antal, University Professor, for his selfless support, without whom I would not have been able to begin my doctoral studies. Throughout the entire period, I could rely on his generous assistance.

I am deeply thankful to Dr. Nikolett Kállai-Szabó, Associate Professor, for her tireless and selfless help, as well as for her guidance and advice. Her expertise, explanations, and endless perseverance were of immense help during my research work.

Furthermore, I would like to thank Dr. Péter Tonka-Nagy, Head of Laboratory, for providing the opportunity to carry out the measurements that formed the basis of my thesis in Department 3 of the Formulation Analytics and Development Laboratory at Egis Pharmaceuticals PLC.

I am grateful to my Parents, Brother, Husband, and Friends, who continuously supported and encouraged me even in the most difficult situations.

Finally, I would like to sincerely thank everyone who contributed in any way to my research work, brainstorming, assisting with measurements, and improving the publications.